

# Sparse Error Localization in Complex Dynamic Networks

Dominik Kahl, Andreas Weber, Maik Kschischo

December 8, 2021

## Abstract

Understanding the dynamics of complex systems is a central task in many different areas ranging from biology via epidemics to economics and engineering. Unexpected behaviour of dynamic systems or even systems failure is sometimes difficult to comprehend. Such unexpected dynamics can be caused by systematic model errors, unknown inputs from the environment and systems faults. Localizing the root cause of these errors or faults and reconstructing their dynamics is only possible if the measured outputs of the system are sufficiently informative. Here, we present a mathematical theory for the measurements required to localize the position of error sources in large dynamic networks. We assume, that faults or errors occur at a limited number of positions in the network. This sparsity assumption facilitates the accurate reconstruction of the dynamic time courses of the errors by solving a convex optimal control problem. For cases, where the sensor measurements are not sufficiently informative to pinpoint the error position exactly, we provide methods to restrict the error location to a smaller subset of network nodes. We also suggest strategies to efficiently select additional measurements for narrowing down the error location.

**E**rrors in complex dynamic systems can be difficult to find. The presence of an error or a fault is detected by the system's unexpected behaviour. Localizing the root cause of the error can, however, be much harder or even impossible. Modern technical devices like cars or planes have dedicated sensors for fault diagnosis or fault isolation. These designs are based on fault detection theory [20, 3], an important research field in control theory. During the design process, engineers specify a set of components whose failure or malfunction must be detected and isolated. To achieve the detectability and isolationability of these prespecified faults, they place sensors with output patterns uniquely indicating a specific type of error. However, there is a trade-off: Increasing the number of errors which can be uniquely isolated requires a larger number of sensors. Indeed, one can show from invertibility theory, that the number of error signals which can uniquely be distinguished is never smaller than the number of sensors required [39, 37, 15, 43, 21].

Finding the root cause of errors or faults is also a crucial task in the analysis of naturally evolved systems such as ecological food webs, biochemical reaction networks or infectious disease models. For example, a protein biomarker like the prostate-specific antigen (PSA) can indicate a disease, here prostate cancer. But, there can be other causes for increased levels of PSA including older age and hyperplasia [31]. A reliable diagnosis requires additional tests, or, stated in engineering terms, the isolation of the fault requires more sensors.

An important difference between engineered and natural or evolved systems is the degree of uncertainty about the interactions between the system's state variables. The couplings between the states of a biochemical reaction network or an ecological food web are usually only partially known. These uncertainties make the development of a useful mathematical model difficult; missing, spurious or misspecified interactions generate structural model errors. Moreover, real world dynamic systems are open, i.e. they receive unknown inputs from their environment. Together, these uncertainties often result in incorrect model predictions. Detection of genuine faults is even harder, if model errors, unknown inputs and faults are interfering. Also, the engineering approach of specifying certain faults in advance is difficult to realize in the case of an incomplete or erroneous model.

In this paper, we provide a mathematical theory for the localization and reconstruction of *sparse* faults and model errors in complex dynamic networks described by ordinary differential equations (ODEs). Sparsity means here, that there is a maximum number of state variables (state nodes)  $k$  affected by an error. Typically,  $k$  is much smaller than the total number of state nodes  $N$ . In contrast to fault isolation approaches [20, 3], we do not require the a priori specification of certain types of faults, but we allow for the possibility that each state node in the network can potentially be targeted by errors (or faults).

The sparse error assumption is often realistic in both the model error and the fault detection context. Faults often affect only a small number of nodes in the network, because the simultaneous failure of several components in a system is unlikely to occur spontaneously. For example, a hardware error or a network failure usually occurs at one or two points in the system, unless the system has been deliberately attacked simultaneously at several different positions. Similarly, gene mutations often affect a restricted number of proteins in a larger signal transduction or gene regulatory network. In the context of model error localization and reconstruction, the sparsity assumption implies that the model is incorrect only at a limited number of positions or, alternatively, that small inaccuracies are ignored and that we focus only on the few (less than  $k$ ) state variables with grossly misspecified governing equations. Throughout this paper, we will exploit the fact that faults, model errors and interactions with the environment can all mathematically be represented as unknown inputs to the system [27, 28, 12, 13, 21]. Thus, we use model error, fault and unknown input as synonyms.

An example for sparse error localization is provided in Fig. 1. The nodes of the network in Fig. 1(a) represent the  $N = 30$  state variables  $\mathbf{x} = (x_1, \dots, x_{30})^T$  of the dynamic system and the edges their interactions. The squares indicate the subset of  $P = 10$  states which are directly measured with output time courses  $\mathbf{y}(t) = (y_1(t), \dots, y_{10}(t))$  plotted in Fig. 1(b). In our simulation, we randomly chose state node  $x_6$  to be affected by an unknown input

$$\mathbf{w}^*(t) = (0, \dots, 0, w_6^*(t), 0, \dots, 0)^T,$$

as highlighted by the wiggly arrow in Fig. 1(a). In reality, the location of this error would be unknown and only the deviations of the output measurements  $\mathbf{y}(t)$  from the expected behaviour would indicate the presence of an error somewhere in the network. Our first result in this paper is a criterion for the localizability of an unknown input in nonlinear systems from output measurements. Based on this, we can decide that a single unknown input ( $k = 1$ ) can be localized and reconstructed from the output data  $\mathbf{y}(t)$ . The estimate  $\hat{\mathbf{w}}(t)$  in Fig. 1(c) provides a satisfying reconstruction of the true input  $\mathbf{w}^*(t)$ . This illustrates our second result: An optimization criterion for the reconstruction of  $k$ -sparse model errors and conditions guaranteeing the accuracy of the reconstruction for linear systems.

In many real world systems, there are practical restrictions on the number or the location of measurements. This restricted set of sensor nodes might render the system non-localizable for a given sparsity  $k$ , i.e. the state nodes (at most  $k$ ) affected by the error or fault cannot exactly be determined from the available output. For example, it is often difficult to measure the dynamic time

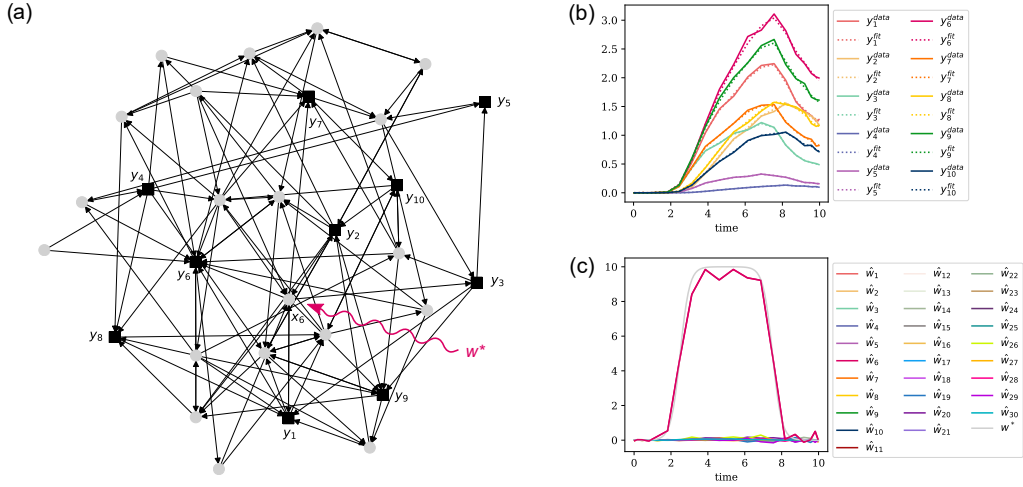


Figure 1: Reconstruction of a sparse unknown input. (a) The influence graph of a linear dynamic system with  $N = 30$  states. The nodes correspond to the state variables and the edges indicate their interactions. The simulated error signal  $\mathbf{w}^*(t) = (0, \dots, 0, w_6^*(t), 0, \dots, 0)^T$  targets the state variable  $x_6$ . The squares indicate the  $P = 10$  sensor nodes providing the output  $\mathbf{y} = (y_1, \dots, y_{10})^T$  (b) The measured output data  $\mathbf{y}^{\text{data}}(t) = (y_1^{\text{data}}(t), \dots, y_{10}^{\text{data}}(t))^T$  (solid lines) can be fitted (dashed lines) by the output  $\hat{\mathbf{y}}(t)$  corresponding to the solution  $\hat{\mathbf{w}}(t)$  (see (c)) of the convex optimal control problem in (24). (c) This estimate  $\hat{\mathbf{w}}(t)$  simultaneously reconstructs the true unknown input  $\mathbf{w}^*(t)$ . One can see, that among the thirty inputs the node  $i = 6$  ( $w_6$ ) was localized as the root cause of the error.

course of a large number of proteins and other molecules in a biochemical reaction network and the root cause for observed errors (e.g. diseases) might be impossible to find. Then, it might still be useful to at least narrow down the location of the errors to subsets of states. As a further result, we present here a coherence measure which quantifies, how difficult it is to distinguish different states as root causes of a  $k$ -sparse error. This coherence measure can be used to cluster states into indistinguishable subsets and to subsequently identify those subsets targeted by model errors.

Once the subsets of the states targeted by errors are known, additional output data are needed to further narrow down the exact error location. We provide an efficient sensor node placement strategy for reducing the uncertainty about the error location. In combination with coherence based output clustering, this sensor selection strategy can be iterated to restrict the exact error location to smaller and smaller subsets until the exact position is isolated.

# Background

## Open dynamic systems with errors and faults

We consider input-output systems of the form

$$\begin{aligned}\dot{\mathbf{x}}(t) &= \mathbf{f}(\mathbf{x}(t)) + \mathbf{w}(t) \\ \mathbf{x}(0) &= \mathbf{x}_0 \\ \mathbf{y}(t) &= \mathbf{c}(\mathbf{x}(t))\end{aligned}\tag{1}$$

where  $\mathbf{x}(t) \in \mathbb{R}^N$  denotes the state of the system at time  $t \in [0, T]$  and  $\mathbf{x}_0 \in \mathbb{R}^N$  is the initial state. The vector field  $\mathbf{f}$  encodes the model of the system and is assumed to be Lipschitz. The function  $\mathbf{c} : \mathbb{R}^N \rightarrow \mathbb{R}^P$  describes the measurement process and maps the system state  $\mathbf{x}$  to the directly observable output  $\mathbf{y}$ .

Model errors or faults are represented as unknown input functions

$$\mathbf{w} : [0, T] \rightarrow \mathbb{R}^N.$$

This ansatz incorporates all types of errors, including missing and wrongly specified interactions, parameter errors [27, 22, 38, 12, 13, 41] as well as faults [20, 3] and unobserved inputs from the environment [21].

The system in (1) can be seen as an input-output map  $\Phi : \mathcal{W} \rightarrow \mathcal{Y}$ ,  $\mathbf{w} \mapsto \mathbf{y}$ . The input space  $\mathcal{W} = \mathcal{W}_1 \oplus \dots \oplus \mathcal{W}_N$  is assumed to be the direct sum of suitable (see below) function spaces  $\mathcal{W}_i$ ,  $i = 1, \dots, N$ . For zero errors  $\mathbf{w} \equiv \mathbf{0}$  (i.e.  $\mathbf{w}(t) = \mathbf{0} \forall t \in [0, T]$ ) we call the system (1) a closed dynamic system. Please note that we do not exclude the possibility of known inputs for control, but we suppress them from our notation.

An error or fault can be detected from the residual

$$\mathbf{r}(t) := \mathbf{y}^{\text{data}}(t) - \mathbf{y}^{(0)}(t)\tag{2}$$

between the measured output data  $\mathbf{y}^{\text{data}}(t)$  and the output  $\mathbf{y}^{(0)}(t) = \Phi(\mathbf{0})(t)$  of the closed system. To infer the model error  $\mathbf{w}(t)$  we have to solve the equation

$$\Phi(\mathbf{w}) = \mathbf{y}^{\text{data}}\tag{3}$$

for  $\mathbf{w}$ . In general, there can be several solutions to the problem (3), unless we either measure the full state of the system or we restrict the set of unknown inputs  $\mathbf{w}$ . In fault detection applications [20, 3], the restriction is given by prior assumptions about the states which are targeted by errors. We will use a sparsity assumption instead. For both cases, we need some notation: Let  $\mathcal{N} = \{1, 2, \dots, N\}$  be the index set of the  $N$  state variables and  $S \subseteq \mathcal{N}$  be a subset

with complement  $S^c = \mathcal{N} \setminus S$ . By  $\mathbf{w}_S(t)$  we indicate the vector function obtained from  $\mathbf{w}(t)$  by setting the entries  $(\mathbf{w}_S)_i$  with  $i \in S^c$  to the zero function. If  $S$  is of minimal cardinality and  $\mathbf{w}_S = \mathbf{w}$  we call  $S$  the *support* of  $\mathbf{w}$ . The corresponding restriction on the input space is defined via

$$\mathcal{W}_S := \{\mathbf{w} \in \mathcal{W} \mid \text{supp } \mathbf{w} \subseteq S\}. \quad (4)$$

Thus,  $S$  characterizes the states  $x_i$  with  $i \in S$  which can *potentially* be affected by a non-zero unknown input  $w_i$ . We will also refer to  $S$  as the set of input or source nodes. The restricted input-output map  $\Phi_S : \mathcal{W}_S \rightarrow \mathcal{Y}$  is again given by (1), but all input components  $\mathbf{w}_i$  with  $i \notin S$  are restricted to be zero functions.

Now, we can formally define invertibility [39, 37]:

**DEFINITION 1:** *The system (1) with input set  $S$  and input-output map  $\Phi$  is called **invertible**, if for two different solutions  $\mathbf{w}^{(1)}, \mathbf{w}^{(2)} \in \mathcal{W}_S$  of (3) and for any data set  $\mathbf{y}^{data} : [0, T] \rightarrow \mathbb{R}^P$  we have*

$$\mathbf{w}^{(1)}(t) - \mathbf{w}^{(2)}(t) = \mathbf{0} \quad (5)$$

*almost everywhere in  $[0, T]$ .*

In other words, invertibility guarantees that (3) with an input set  $S$  has only one solution  $\mathbf{w}^*$  (up to differences of measure zero), which corresponds to the true model error. In the following, we mark this true model error with an asterisk, while  $\mathbf{w}$  without asterisk denotes an indeterminate input function.

## Structural Invertibility and Independence of Input Nodes

There are several algebraic or geometric conditions for invertibility [39, 37, 15, 14, 1], which are, however, difficult to test for large systems and require exact knowledge of the systems equations (1), including all the parameters. *Structural invertibility* of a system is prerequisite for its invertibility and can be decided from a graphical criterion [43], see also Theorem 3 below. Before, we define the influence graph (see e.g. [23])

**DEFINITION 2:** *The **influence graph**  $g = (\mathcal{N}, \mathcal{E})$  of the system (1) is a digraph, where the set of nodes  $\mathcal{N} = \{1, 2, \dots, N\}$  represents the  $N$  state variables  $\mathbf{x} = (x_1, \dots, x_N)$  and the set of directed edges  $\mathcal{E} = \{i_1 \rightarrow l_1, i_2 \rightarrow l_2, \dots\}$  represents the interactions between those states in the following way: There is a directed edge  $i \rightarrow l$  for each pair of state nodes  $i, l \in \mathcal{N}$  if and only if  $\frac{\partial f_l}{\partial x_i}(\mathbf{x}) \neq 0$  for some  $\mathbf{x}$  in the state space  $\mathcal{X}$ .*

In addition to the set of input nodes  $S \subseteq \mathcal{N}$  we define the output nodes  $Z \subseteq \mathcal{N}$  of the system in (1). The latter are determined by the measurement function  $\mathbf{c}$ . Without restriction of generality we assume in the following that a subset  $Z \subseteq \{1, 2, \dots, N\}$  of  $P$  state nodes are sensor nodes, i.e. they can directly be measured, which corresponds to  $c_i(\mathbf{x}) = x_i$  for  $i \in Z$ . All states  $x_l$  with  $l \notin Z$  are not directly monitored.

A necessary criterion for structural invertibility is given by the following graphical condition [43]:

**THEOREM 3:** *Let  $g = (\mathcal{N}, \mathcal{E})$  be an influence graph and  $S, Z \subseteq \mathcal{N}$  be known input and output node sets with cardinality  $M = \text{card}S$  and  $P = \text{card}Z$ , respectively. If there is a family of directed paths  $\Pi = \{\pi_1, \dots, \pi_M\}$  with the properties*

1. *each path  $\pi_i$  starts in  $S$  and terminates in  $Z$ ,*
2. *any two paths  $\pi_i$  and  $\pi_j$  with  $i \neq j$  are node-disjoint,*

*then the system is structurally invertible. If such a family of paths exists, we say  $S$  is **linked in  $g$  into  $Z$** .*

In the Appendix we discuss why we have the strong indication that this theorem provides also a sufficient criterion for structural invertibility up to some pathological cases.

A simple consequence of this theorem is that for an invertible system, the number  $P$  of sensor nodes cannot be smaller than the number of input nodes  $M$ . This is the reason, why for fault detection the set of potentially identifiable error sources  $S$  is selected in advance [3]. Without a priori restriction on the set of potential error sources, we would need to measure all states. Please note, that there are efficient algorithms to check, whether a system with a given influence graph  $g$  and given input and sensor node set  $S$  and  $Z$  is invertible (see [21] for a concrete algorithm and references therein).

## **Independence of Input Nodes**

If the path condition for invertibility in Theorem 3 is fulfilled for a given triplet  $(S, g, Z)$  we can decide, whether the unknown inputs targeting  $S$  can be identified in the given graph  $g$  using the set of sensor nodes  $Z$ . Without a priori knowledge about the model errors, however, the input set  $S$  is unknown as well. Therefore, we will consider the case that the input set  $S$  is unknown in the results section. To this end, we define an independence structure on the union of all possible input sets:

DEFINITION 4: The triple  $\Gamma := (\mathcal{L}, g, Z)$  consisting of an influence graph  $g = (\mathcal{N}, \mathcal{E})$ , and **input ground set**  $\mathcal{L} \subseteq \mathcal{N}$ , and an output set  $Z$  is called a **gammoid**. A subset  $S \subseteq \mathcal{L}$  is understood as an input set. An input set  $S$  is called **independent in  $\Gamma$** , if  $S$  is linked in  $g$  into  $Z$ .

The notion of (linear) independence of vectors is well known from vector space theory. For finite dimensional vector spaces, there is the rank-nullity theorem relating the dimension of the vector space to the dimension of the null space of a linear map. The difference between the dimension of the vector space and the null space is called the rank of the map. The main advantage of the gammoid interpretation lies in the following rank-nullity concept:

DEFINITION 5: Let  $\Gamma = (\mathcal{L}, g, Z)$  be a gammoid.

1. The **rank** of a set  $S \subseteq \mathcal{L}$  is the size of the largest independent subset  $\tilde{S} \subseteq S$ .
2. The **nullity** is defined by the rank-nullity theorem

$$\text{rank}S + \text{null}S = \text{card}S. \quad (6)$$

Note, that the equivalence of a consistent independence structure and a rank function (see definition 5 1.) as well as the existence of a rank-nullity theorem (see definition 5 2.) goes back to the early works on matroid theory [44]. It has already been shown [33], that the graph theoretical idea of linked sets (see definition 4) fulfils the axioms of matroid theory and therefore inherits its properties. The term gammoid for such a structure of linked sets was probably first used in [35] and since then investigated under this name, with slightly varying definitions. We find the formulation above to be suitable for our purposes (see also the SI Appendix for more information about gammoids).

## Results

Here, we consider the localization problem, where the input set  $S$  is unknown. However, we make a sparsity assumption by assuming that  $S$  is a small subset of the ground set  $\mathcal{L} \subseteq \mathcal{N}$ . Depending on the prior information, the ground set can be the set of all state variables  $\mathcal{N}$  or a subset.

The sparsity assumption together with the definition of independence of input nodes in Definitions 4 and 5 can be exploited to generalize the idea of sparse sensing [10, 6, 9, 46] to the solution of the dynamic problem (3). Sparse sensing for matrices is a well established field in signal and image processing (see e.g. [46, 16]). There are, however, some nontrivial differences: First, the input-output map  $\Phi$  is not necessarily linear. Second, even if  $\Phi$  is linear, it is



a compact operator between infinite dimensional vector spaces and therefore the inverse  $\Phi^{-1}$  is not continuous. This makes the inference of unknown inputs  $\mathbf{w}$  an ill-posed problem, even if (3) has a unique solution [17].

## Sparse Error Localization and Spark

Definition 4 enables us to transfer the concept of the *spark* [10] to dynamic systems:

DEFINITION 6: *Let  $\Gamma = (\mathcal{L}, g, Z)$  be a gammoid. The **spark** of  $\Gamma$  is defined as the largest integer, such that for each input set  $S \subseteq \mathcal{L}$*

$$\text{card}S < \text{spark}\Gamma \Rightarrow \text{null}S = 0. \quad (7)$$

Let's assume we have a given dynamic system with influence graph  $g = (\mathcal{N}, \mathcal{E})$  and with an output set  $Z \subset \mathcal{N}$ . In addition, we have chosen an input ground set  $\mathcal{L}$ . Together, we have the gammoid  $\Gamma = (\mathcal{L}, g, Z)$ . The spark gives the smallest number of inputs that are dependent. As for the compressed sensing problem for matrices [10], we can use the spark to check, under which condition a sparse solution is unique:

THEOREM 7: *For an input  $\mathbf{w}$  we denote  $\|\mathbf{w}\|_0$  the number of non-zero components. Assume  $\mathbf{w}$  solves (3). If*

$$\|\mathbf{w}\|_0 < \frac{\text{spark}\Gamma}{2}, \quad (8)$$

*then  $\mathbf{w}$  is the unique sparsest solution.*

This theorem provides a necessary condition for the localizability of a  $k$ -sparse error in a nonlinear dynamic system. For instance, if we expect an error or input to target a single state node like in Fig. 1(a), we have  $\|\mathbf{w}^*\|_0 = 1$  and we need  $\text{spark}\Gamma \geq 3$  to pinpoint the exact position of the error in the network. If an edge in the network is the error source, then two nodes are affected and  $\|\mathbf{w}^*\|_0 = 2$ . Such an error could be a misspecified reaction rate in a biochemical reaction or a cable break in an electrical network. To localize such an error we need  $\text{spark}\Gamma \geq 5$ .

For smaller networks like the one in Fig. 1(a), it is possible to exactly compute the spark (Definition 6) of a gammoid (Definition 4) using a combinatorial algorithm iterating over all possible input node sets. However, the computing time grows rapidly with the size of the network. Below we present bounds for the spark, which can efficiently be computed.

## Convex Optimization for Sparse Input Reconstruction

As in compressed sensing for matrices, finding the solution of (3) with a minimum number of non-zero components  $\|\mathbf{w}\|_0$  is an NP-hard combinatorial problem. Here, we formulate a convex optimal control problem as a relaxed version of this combinatorial problem. We define a Restricted-Isometry-Property (RIP) [6] for the input-output operator  $\Phi$  defined by (1) and provide conditions for the exact sparse recovery of errors in linear dynamic systems by solutions of the relaxed problem. As a first step it is necessary to introduce a suitable norm promoting the sparsity of the vector of input functions  $\mathbf{w}(t)$ .

Say,  $\mathcal{L}$  is an input ground set of size  $L$ . The space of input functions

$$\mathcal{W} := \bigoplus_{i \in \mathcal{L}} \mathcal{W}_i \quad (9)$$

is composed of all function spaces  $\mathcal{W}_i$  corresponding to input component  $w_i$ . By definition of the input ground set,  $w_i \equiv 0$  for  $i \notin \mathcal{L}$ . Thus  $\mathcal{W}_i = \{0\}$  for  $i \notin \mathcal{L}$ . Assume, that each function space  $\mathcal{W}_i = L^p([0, T])$  is a Lebesgue space equipped with the  $p$ -norm

$$\|w_i\|_p = \left( \int_0^T |w_i(t)|^p dt \right)^{1/p}. \quad (10)$$

We indicate the vector

$$\underline{\mathbf{w}} := \begin{pmatrix} \|w_1\|_p \\ \vdots \\ \|w_L\|_p \end{pmatrix} \in \mathbb{R}^L \quad (11)$$

collecting all the component wise function norms by an underline. Taking the  $q$ -norm in  $\mathbb{R}^L$

$$\|\underline{\mathbf{w}}\|_q = (\underline{w}_1^q + \dots + \underline{w}_L^q)^{1/q} \quad (12)$$

of  $\underline{\mathbf{w}}$  yields the  $p$ - $q$ -norm on  $\mathcal{W}$

$$\|\mathbf{w}\|_q := \|\underline{\mathbf{w}}\|_q. \quad (13)$$

The parameter  $p$  appears implicitly in the underline. Since our results are valid for all  $p \in [1, \infty)$ , we will suppress it from the notation.

Similarly, for the  $P$  outputs of the system, the output space

$$\mathcal{Y} = \mathcal{Y}_1 \oplus \dots \oplus \mathcal{Y}_P. \quad (14)$$

can be equipped with a  $p$ - $q$ -norm

$$\|\mathbf{y}\|_q := \|\underline{\mathbf{y}}\|_q. \quad (15)$$

An important subset of the input space  $\mathcal{W}$  is the space  $\Sigma_k$  of  $k$ -sparse inputs

$$\mathbf{w} \in \Sigma_k \Rightarrow \|\mathbf{w}\|_0 \leq k. \quad (16)$$

In analogy to a well known property [6] from compressed sensing we define for our dynamic problem:

**DEFINITION 8:** *The **Restricted-Isometry-Property (RIP)** of order  $2k$  is fulfilled, if there is a constant  $\delta_{2k} \in (0, 1)$  such that for any two vector functions  $\mathbf{u}, \mathbf{v} \in \Sigma_k$  the inequalities*

$$(1 - \delta_{2k})\|\underline{\mathbf{u}} - \underline{\mathbf{v}}\|_2^2 \leq \|\underline{\Phi(\mathbf{u})} - \underline{\Phi(\mathbf{v})}\|_2^2 \quad (17)$$

and

$$\|\underline{\Phi(\mathbf{u})} + \underline{\Phi(\mathbf{v})}\|_2^2 \leq (1 + \delta_{2k})\|\underline{\mathbf{u}} + \underline{\mathbf{v}}\|_2^2 \quad (18)$$

hold.

The reconstruction of sparse unknown inputs can be formulated as the optimization problem

$$\text{minimize } \|\mathbf{w}\|_0 \text{ subject to } \|\Phi(\mathbf{w}) - \mathbf{y}^{\text{data}}\|_2 \leq \epsilon \quad (19)$$

where  $\epsilon > 0$  incorporates uniform bounded measurement noise. A solution  $\hat{\mathbf{w}}$  of this problem will reproduce the data  $\mathbf{y}^{\text{data}}$  according to the dynamic equations (1) of the system with a minimal set of nonzero components, i.e., with a minimal set  $S$  of input nodes. As before, finding this minimal input set is a NP-complete problem. Therefore, let us consider the relaxed problem

$$\text{minimize } \|\mathbf{w}\|_1 \text{ subject to } \|\Phi(\mathbf{w}) - \mathbf{y}^{\text{data}}\|_2 \leq \epsilon. \quad (20)$$

The following result implies, that for a linear system of ODEs with  $\mathbf{f}(\mathbf{x}) = \mathbf{A}\mathbf{x}$  and  $\mathbf{c}(\mathbf{x}) = \mathbf{C}\mathbf{x}$  with matrices  $\mathbf{A} \in \mathbb{R}^{N \times N}$  and  $\mathbf{C} \in \mathbb{R}^{P \times N}$  in (1) the optimization problem (20) has a unique solution.

**THEOREM 9:** *If  $\Phi$  is linear, then (20) is a convex optimization problem.*

For a given input vector  $\mathbf{w} \in \mathcal{W}$  we define the best  $k$ -sparse approximation in  $q$ -norm as [16]

$$\sigma_k(\mathbf{w})_q := \min_{\mathbf{u} \in \Sigma_k} \|\mathbf{w} - \mathbf{u}\|_q \quad (21)$$

i.e. we search for the function  $\mathbf{u}$  that has minimal distance to the desired function  $\mathbf{w}$  under the condition that  $\mathbf{u}$  has at most  $k$  non-vanishing components. If  $\mathbf{w}$  is  $k$ -sparse itself, then we can choose  $\mathbf{u} = \mathbf{w}$  and thus the distance between the approximation and the desired function vanishes,  $\sigma_k(\mathbf{w})_q = 0$ .

**THEOREM 10:** *Assume  $\Phi$  is linear and the RIP of order  $2k$  holds. Let  $\mathbf{w}^*$  be the solution of (19). The optimal solution  $\hat{\mathbf{w}}$  of (20) obeys*

$$\|\hat{\mathbf{w}} - \mathbf{w}^*\|_2 \leq C_0 \frac{\sigma_k(\mathbf{w}^*)_1}{\sqrt{k}} + C_2 \epsilon \quad (22)$$

with non-negative constants  $C_1$  and  $C_2$ <sup>1</sup>.

Motivated by the latter theorem we define a cost functional

$$J[\mathbf{w}] := \frac{1}{2} \|\Phi(\mathbf{w}) - \mathbf{y}^{\text{data}}\|_2^2 + \beta \|\mathbf{w}\|_1 \quad (23)$$

with given data  $\mathbf{y}^{\text{data}}$  and regularization constant  $\beta$ . The solution of the optimization problem in Lagrangian form

$$\text{minimize } J[\mathbf{w}] \text{ subject to (1),} \quad (24)$$

provides an estimate for the input  $\hat{\mathbf{w}}$ , see Fig. 1 for an example.

## Coherence of potential input nodes in linear systems

So far we have given theorems for the localizability and for the reconstruction of sparse errors in terms of the spark and RIP. However, computing the spark or checking whether the RIP condition holds are again problems whose computation time grows rapidly with increasing systems size. Now, we present a coherence measure between a pair of state nodes  $i, j$  in linear systems indicating how difficult it is to decide whether a detected error is localized at  $i$  or at  $j$ . The coherence provides a lower bound for the spark and can be approximated by an efficient shortest path algorithm. Computing the coherence for each pair

<sup>1</sup>Formulas for the constants  $C_1$  and  $C_2$  can be found in the supplemental material.

of state nodes in the network yields the coherence matrix, which can be used to isolate a subset of states where the root cause of the error must be located.

If the system (1) is linear, i.e.  $\mathbf{f}(\mathbf{x}) = A\mathbf{x}$  and  $\mathbf{c}(\mathbf{x}) = C\mathbf{x}$ , we can use the Laplace-transform

$$T(s)\tilde{\mathbf{w}}(s) = \tilde{\mathbf{y}}(s), \quad s \in \mathbb{C} \quad (25)$$

to represent the input-output map  $\Phi_{\mathcal{L}}$  by the  $L \times P$ -transfer matrix  $T(s)$ . The tilde denotes Laplace-transform. Again, we assume that  $w_i \equiv 0$  for all  $i \notin \mathcal{L}$  and  $\tilde{\mathbf{w}}(s)$  is the vector of Laplace transforms of the components of  $\mathbf{w}$  which are in the ground set  $\mathcal{L}$ . Recall that  $L \leq N$  is the number of states in the ground set  $\mathcal{L}$  and  $P$  the number of measured outputs. As before,  $\mathcal{L} = \mathcal{N}$  is still a possible special case.

We introduce the input gramian

$$G(s) := T^*(s)T(s) \quad (26)$$

where the asterisk denotes the hermitian conjugate. Note, that the input gramian is a  $L \times L$  matrix. Assume that we have chosen an arbitrary but fixed numbering of the states in the ground set, i.e.  $\mathcal{L} = \{l_1, \dots, l_L\}$  is ordered.

**DEFINITION 11:** *Let  $G$  be the input gramian of a linear dynamic system. We call*

$$\mu_{ij}(s) := \frac{|G_{ij}(s)|}{\sqrt{G_{ii}(s)G_{jj}(s)}}, \quad s \in \mathbb{C} \quad (27)$$

*the **coherence function** of state nodes  $l_i$  and  $l_j$ . We call*

$$\mu(s) := \max_{i \neq j} \mu_{ij}(s) \quad (28)$$

*the **mutual coherence** at  $s \in \mathbb{C}$ .*

Coherence measures to obtain lower bounds for the spark have been used for signal decomposition [11] and compressed sensing for matrices [10]. In the next theorem, we use the mutual coherence for linear dynamic systems in a similar way to provide bounds for the spark.

**THEOREM 12:** *Let  $\Gamma = (\mathcal{L}, g, Z)$  be a gammoid with mutual coherence  $\mu(s)$  at some point  $s \in \mathbb{C}$ . then*

$$\text{spark}\Gamma \geq \frac{1}{\mu(s)} + 1 \quad \forall s \in \mathbb{C}. \quad (29)$$

Since (29) is valid for all values of  $s \in \mathbb{C}$ , it is tempting to compute  $\inf_{s \in \mathbb{C}} \mu(s)$  to tighten the bound as much as possible. Please note, however, that  $\mu(s)$  is not a holomorphic function and thus the usual trick of using a contour in the complex plane and applying the maximum/minimum modulus principle can not be applied (see e.g. [40]). Instead, we will introduce the shortest path coherence, which can efficiently be computed and which can be used in Theorem 12 to obtain lower bounds for the spark.

## Shortest Path Coherence

There is a one-to-one correspondence between linear dynamic systems and weighted<sup>2</sup> gammoids. The weight of the edge  $j \rightarrow i$  is defined by the Jacobian matrix

$$F(j \rightarrow i) := \frac{\partial f_i(\mathbf{x})}{\partial x_j} \quad (30)$$

and is constant for a linear system. We extend this definition to sets of paths in the following way: Denote by  $\pi = (i_0 \rightarrow i_1 \rightarrow \dots \rightarrow i_\ell)$  a directed path in the influence graph  $g$ . The length of  $\pi$  is  $\text{len}(\pi) = \ell$  and the weight of  $\pi$  is given by the product of all edge weights along that path:

$$F(\pi) = \prod_{k=1}^{\ell} F(i_{k-1} \rightarrow i_k). \quad (31)$$

Let  $\Pi = \{\pi_1, \dots, \pi_M\}$  be a set of paths. The weight of  $\Pi$  is given by the sum of all individual path weights:

$$F(\Pi) = \sum_{k=1}^M F(\pi_k). \quad (32)$$

The input gramian  $G(s)$  (26) is the composition of the transfer function  $T$  and its hermitian conjugate  $T^*$ . The transfer function  $T$  can be interpreted as a gammoid  $\Gamma = (\mathcal{L}, g, Z)$ , where the input nodes from  $\mathcal{L}$  correspond to the columns of  $T$  and the output nodes from  $Z$  correspond to the rows of  $T$ .

There is also a *transposed gammoid*<sup>3</sup>.

$$\Gamma' = (Z', g', \mathcal{L}'). \quad (33)$$

corresponding to the hermitian conjugate  $T^*$ , see Fig. 2. Here, the *transposed graph*  $g'$  is obtained by flipping the edges of the original graph  $g$ . The input

<sup>2</sup>Weights are understood as real constant numbers.

<sup>3</sup>The transposed gammoid should not be confused with the notion of a dual gammoid in matroid theory [44].

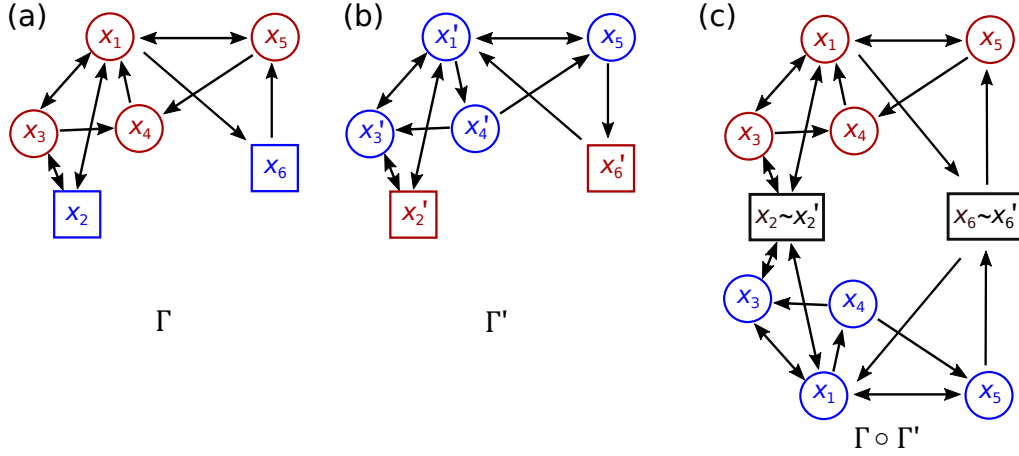


Figure 2: Gammoid representation of the input gramian. (a) An exemplary gammoid  $\Gamma$ . The nodes in red represent the input ground set  $\mathcal{L}$  and the nodes in blue (squares) the output set  $Z$ . (b) The transposed gammoid  $\Gamma'$ . Compared to (a), the arrows are flipped. The red nodes (squares) represent the input ground set  $Z'$  and the nodes in blue the output set  $\mathcal{L}'$ . (c) The combined gammoid ( $\Gamma \circ \Gamma'$ ). The outputs  $Z$  of  $\Gamma$  are identified with the inputs  $Z'$  of  $\Gamma'$ . Again, red nodes represent the inputs  $\mathcal{L}$  and the blue nodes represent the outputs  $\mathcal{L}'$  of the gammoid ( $\Gamma \circ \Gamma'$ ).

ground set  $Z'$  of the transposed gammoid  $\Gamma'$  corresponds to the output set  $Z$  of  $\Gamma$ . Similarly, the output set  $\mathcal{L}'$  of  $\Gamma'$  is given by the input ground set  $\mathcal{L}$  of  $\Gamma$ .

As we have gammoid representations  $\Gamma$  and  $\Gamma'$  for  $T$  and  $T^*$ , also the gramian has such a gammoid representation which we denote as  $(\Gamma \circ \Gamma')$ . To obtain  $(\Gamma \circ \Gamma')$  we identify the outputs  $Z$  of  $\Gamma$  with the inputs  $Z'$  of  $\Gamma'$ , see Fig. 2(c).

**DEFINITION 13:** Let  $\Gamma$  be a weighted gammoid with ground set  $\mathcal{L} = \{l_1, \dots, l_L\}$ . For two nodes  $l_i, l_j \in \mathcal{L}$  let  $\psi_{ij}$  denote the shortest path from  $l_i$  to  $l'_j$  in  $(\Gamma \circ \Gamma')$ . We call

$$\mu_{ij}^{short} := \frac{|F(\psi_{ij})|}{\sqrt{F(\psi_{ii})F(\psi_{jj})}} \quad (34)$$

the shortest path coherence between  $l_i$  and  $l_j$ .

**THEOREM 14:** We find that

$$\mu_{ij}^{short} \geq \lim_{|s| \rightarrow \infty} \frac{|G_{ij}(s)|}{\sqrt{G_{ii}(s)G_{jj}(s)}}. \quad (35)$$

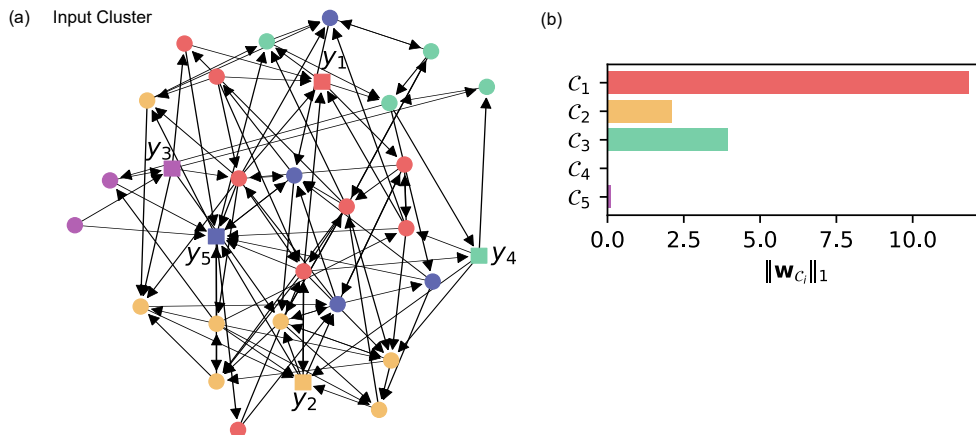


Figure 3: Restricting the error location to a subset of state nodes. (a) The graph of a linear dynamic system with 30 nodes and 5 output nodes  $y_1, \dots, y_5$ . These outputs are not sufficient to pinpoint the state  $x_6$  as the single root cause of the unknown input  $w^*(t) = (0, \dots, 0, w_6^*(t), 0, \dots, 0)^T$ . The 5 different colours of the state nodes indicate their membership in one of the different input clusters  $\mathcal{C}_1, \dots, \mathcal{C}_5$ . State nodes within the same input cluster can not be distinguished from each other as possible error sources. (b) The sum over signal norms of each state in an input cluster (see (37)) can be used as an indicator that at least one node in this particular cluster is targeted by an error. The barplot indicates that  $\mathcal{C}_1$  is the cluster most likely to be targeted by a 1-sparse error.

We see that

$$\inf_{s \in \mathcal{C}} \max_{i \neq j} \mu_{ij}(s) \leq \max_{i \neq j} \mu_{ij}^{\text{short}} \quad (36)$$

and therefore the shortest path mutual coherence can also be used in theorem 12 to get a (more pessimistic) bound for the spark. The advantage of the shortest shortest path mutual coherence is that it can readily be computed even for large ( $N > 100$ ) networks.

## Examples and Node Clustering

In this section we illustrate by example, how our theoretical results from the previous section can be used to localize and reconstruct unknown inputs. These inputs can be genuine inputs from the environment or model errors or faults in a dynamic system [13, 21].



### Example 1: Reconstruction of the root cause of a sparse error

We are now coming back to the scenario in Fig.1. Assume, we have detected some unexpected output behaviour in a given dynamic system. Now, we want to reconstruct the root cause for the detected error. We simulated this scenario for a linear system with  $N = 30$  state nodes  $\mathcal{N} = \{1, \dots, 30\}$  and randomly sampled the interaction graph  $g$ , see again Fig.1(a). The outputs are given as time course measurements  $y_1^{data}(t), \dots, y_{10}^{data}(t)$  of  $P = 10$  randomly selected sensor nodes  $Z$ , see Fig.1(b). In our simulation, we have added the unknown input  $w^*(t)$  with the only nonzero component  $w_6^*(t)$  (Fig.1(c)). However, we assume that we have no information about the localization of this unknown input. Thus, the ground set is  $\mathcal{L} = \mathcal{N}$ .

For a network of this size, it is still possible to exactly compute the spark (Definition 6) of the gammoid  $(\mathcal{L}, g, Z)$  (Definition 4). This straightforward algorithm iterates over two different loops: In the inner loop we iterate over all possible input sets  $S$  of size  $r$  and check, whether  $S$  is linked in  $g$  into  $Z$  (see Theorem 3). In the outer loop we repeat this for all possible  $r = 1, 2, \dots, N$ . The algorithm terminates, if we find an input set which is not linked into  $Z$ . If  $r$  is largest subset size for which all  $S$  are linked in  $g$  into  $Z$ , the spark is given by  $r + 1$ .

For the network in Fig.1(a) we find that spark  $\Gamma = 3$ . From (8) we conclude, that an unknown input targeting a single node in the network can uniquely be localized. Thus, under the assumption that the output residual was caused by an error targeting a single state node, we can uniquely reconstruct this input from the output. The reconstruction is obtained as the solution of the regularized optimization problem in (24), see Fig.1(c). For the fit we allowed each node  $x_i$  to receive an input  $\hat{w}_i$ . We used a regularization constant of  $\beta = 0.01$  in (24).

Please note, that a necessary condition for the reconstruction to work is an assumption about the sparsity of the unknown input. If we would assume that more than one state node is targeted by an error, we would need a larger spark to exactly localize and reconstruct the error. This would either require a smaller ground set  $\mathcal{L}$  or a different set of sensor nodes  $Z$ , or both.

### Example 2: Restricting the error location to a subset of state nodes

In Fig. 3 we have plotted the graph corresponding to the same system as in Fig. 1, but now with a different set of only 5 output nodes  $Z$ . As before, we performed a twin experiment by adding an error signal  $w_6^*(t)$  to the state node  $i = 6$  only. However, this smaller sensor node set  $Z$  is not sufficient to localize even a single error at an unknown position. The corresponding gammoid  $\Gamma = (\mathcal{L}, g, Z)$  with ground set  $\mathcal{L} = \mathcal{N}$  has spark  $\Gamma = 2$  and therefore the condition

(8) is not fulfilled. Solving the optimization problem (20) with  $\mathcal{L}$  as a ground set is also not guaranteed to reconstruct the localization of the unknown input, since the RIP condition (Theorem 10) cannot practically be tested.

Nevertheless, we can still restrict the position of the error using a node clustering strategy: We use the shortest path coherence matrix ( $\mu_{ij}^{\text{short}}$ ) as a similarity index between each pair  $(i, j) \in \mathcal{N} \times \mathcal{N}$  of state nodes and employ a standard hierarchical clustering algorithm to group the state nodes in  $\mathcal{L}$  into disjoint input clusters  $\mathcal{C}_1, \dots, \mathcal{C}_5$  such that  $\mathcal{L} = \mathcal{C}_1 \dot{\cup} \mathcal{C}_2 \dot{\cup} \dots \dot{\cup} \mathcal{C}_5$ . The nodes belonging to one and the same cluster have such a high coherence that it is not possible to determine which of them is the root course of the error. But, as can be seen in Fig. 2(b), we can rank the input clusters to at least isolate the cluster containing the node targeted by the error. To this end, we solve the optimal control problem (24) and sum the estimated hidden inputs within each cluster

$$\|\mathbf{w}_{\mathcal{C}_k}\|_1 = \sum_{i \in \mathcal{C}_k} \|w_i\|_p. \quad (37)$$

The strongest total input signal is observed for cluster  $\mathcal{C}_1$ . If we assume that the root cause of the observed error is localized at a single state node (sparsity  $k = 1$ ), we select this cluster  $\mathcal{C}_1$ . This corresponds to the ground truth in this twin experiment. However, if we suspect more than one node to be targeted by errors (say  $k \geq 2$ ) but the strongest cluster contains less than  $k$  nodes, we have to consider more clusters in the order of their ranking until  $k$  nodes are covered.

### Example 3: Sensor node selection and a strategy for constricting the error location

The clustering of the input ground set described in the previous Example 2 is always dependent on the given output set  $Z$ . This implies that the size and location of the input clusters in the last example depends on the output set  $Z$ . To further narrow down the position of the single unknown input in Fig. 2, additional or more carefully chosen measurements are necessary. A set  $Z$  of sensor nodes is most effective, if the sensors provide output signals with distinct information. We will describe now by example, how the degree of coherence between the output measurements can be quantified. This will provide a strategy for selecting incoherent, i.e. non-redundant, sensor nodes.

In the same way we use  $(\Gamma \circ \Gamma')$  to compute a measure for the indistinguishability of input nodes, we can compute the shortest path coherence matrix of  $(\Gamma' \circ \Gamma)$  to quantify the indistinguishability of output nodes. This output coherence measure depends on the chosen input set. Since we have already identified  $\mathcal{C}_1$  as the target cluster for the error (see Fig. 3), we now restrict the input set

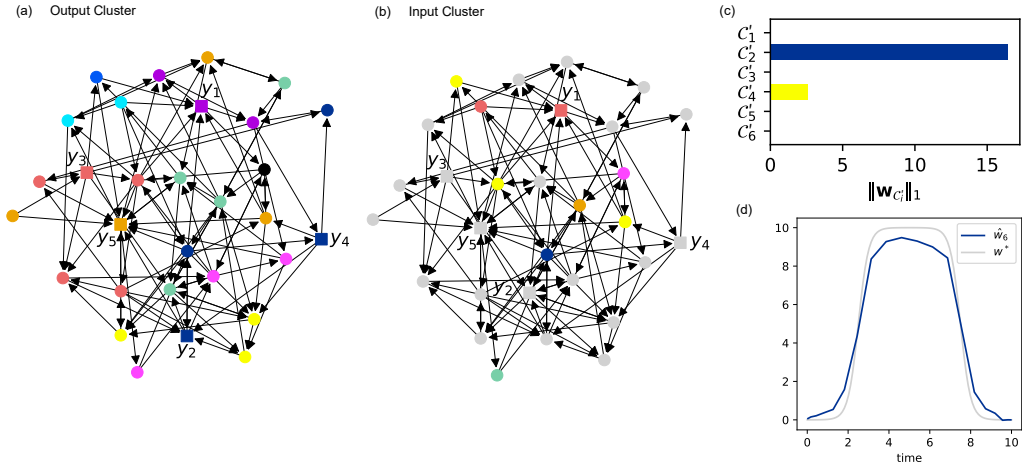


Figure 4: Narrowing down the location of the error using informative sensor nodes. (a) The system, the unknown inputs and the output node set are the same as in Fig. 3. But, the colours in this graph indicate now clusters of coherent *outputs*. Measuring more than one state node within the same output cluster does not provide additional information about the location of the error as compared to a single measurement in each cluster. For example, output sensors  $y_2$  and  $y_4$  are in the same output cluster and thus provide only redundant information. Therefore, we move the sensor  $y_2$  to an output cluster which is not yet covered by a sensor. (b) *Input* clustering after moving  $y_2$ . The state nodes within each of the 6 input clusters can still not be distinguished as the cause of the error. (c) Cluster  $\mathcal{C}'_2$  in (b) (a subcluster of the original  $\mathcal{C}_1$  in Fig. 3) has the largest total signal norm ((37)). In this example,  $\mathcal{C}'_2$  consists only of the single state node with  $i = 6$ . (d) The reconstructed output  $\hat{u}_6(t)$  is a good estimate of the true error signal.

to  $\mathcal{C}_1$  and compute the output coherence with respect to this restricted ground set  $\mathcal{C}_1$ . Fig. 4(a) shows the resulting clusters of indistinguishable output nodes. Sensor nodes in the same output cluster provide similar, and thus redundant information. Hence, it makes sense to place the sensors in distinct output clusters.

We can see in Fig. 4(a) that the sensors  $y_2$  and  $y_4$  lie in the same output cluster. To collect complementary information about the location of the unknown input, we replace one of these two sensors, say  $y_2$ , by a sensor in a different cluster. In Fig. 4(b), the output  $y_2$  was moved to a different position and thus covers a different output cluster. We can now repeat the input clustering from Example 2 for the gammoid with  $\mathcal{C}_1$  as input ground set and our improved output set. The resulting input clustering can be seen in Fig. 4(b). The grey nodes represent the state variables which are not in the input ground set and therefore not considered in the clustering. With  $\mathcal{C}_1$  as input ground set we can again solve the optimization problem (24) and add the input norms (see (37)) in each of the new subclusters of  $\mathcal{C}_1$ . From Fig. 4(c) we identify the new cluster  $\mathcal{C}'_2$  (a subcluster of the original  $\mathcal{C}_1$ ) as the target cluster for unknown inputs. In this example,  $\mathcal{C}'_2$  consists only of the single state node with  $i = 6$ . Indeed, this is correct input node in our twin experiment. Solving the optimization problem one last time with only the single node target cluster  $\mathcal{C}'_2 = \{6\}$  as ground set provides again an accurate reconstruction  $\hat{w}_6(t)$  of the error signal, see Fig. 4(d).

This example illustrates, how the input ground set can be more and more reduced by iteratively repeating the strategy consisting of input node clustering, target cluster selection using convex optimization, output clustering and non-redundant sensor node placement.

Please note, that this strategy depends on the assumption of sparsity. Here, we assumed a single input, i.e. a sparsity of  $k = 1$ . However, it is straightforward to generalize to  $k \geq 2$  sparse errors, as long as these potential target clusters cover at least  $k$  potential input nodes. Also note, that in the case of real data with stochastic input noise, there might be several clusters with almost the same total input signal. Then, it might be reasonable to also consider clusters with approximately the same total input. Analysing the effect of stochastic measurement noise is left as a question for further research.

## Discussion

Finding the root cause of errors or faults is important in many contexts. We have presented a mathematical theory for the localization of sparse errors, which overcomes the need to a priori assume certain types of errors. This restriction is replaced by the sparsity assumption, which is plausible in many real world

settings, where the failure of a small number of components is observed from the sensors, but the localization of the fault is unknown. Similarly, for the problem of modelling dynamic systems, it is important to know where the model is wrong and which states in the model need a modified description. This includes also open systems, which are influenced by unknown inputs from their environment. We have used the gammoid concept to define the notion of independence for inputs to dynamic systems. This allowed us to generalize concepts from sparse sensing to localize and infer such sparse unknown inputs.

Theorem 7 is general and applies to nonlinear systems. The other results are only proved for linear systems. An important open research question is to check, whether the optimization problem in (20) is also suitable for nonlinear systems. In addition, the RIP-condition in Definition 8 is already hard to test for linear systems, a situation we already know from classical compressed sensing for matrices [46]. However, there is an additional complication in the problem of estimating the inverse of the input-output map  $\Phi$  corresponding to the dynamic system (1) : The map  $\Phi$  is compact and maps from an infinite dimensional input space to the infinite dimensional output space. Inverse systems theory [17] tells us, that the inversion of such operators is discontinuous. Thus, more research on the numerics of this  $L_1$  regularized optimal control problem is needed [42]. In addition, stochastic dynamic systems with unknown inputs will provide an interesting direction for further research.

Our results are complementary to recent work on Data-Driven Dynamic Systems, where the the goal is to discover the dynamics solely from measurement data [4, 45, 32, 8]. For data sets of limited size, these purely data driven methods might profit from the prior knowledge encoded by an possibly imperfect but informative model. Our work provides a straightforward approach to combine models and data driven methods. For a given model, the estimated error signals can be analysed with a data driven method to discover their inherent dynamics. We believe that the combination of data driven systems with the prior information from interpretable mechanistic models will provide major advances in our understanding of dynamic networks.

## Acknowledgements

The authors would like to thank Philipp Wendlandt and Jörg Zimmermann for the valuable discussions throughout the creation process. The present work is part of the SEEDS project, funded by *Deutsche Forschungsgemeinschaft (DFG)*, project number 354645666.

## A Spaces and Norms

Our gammoid approach enables us to generalize concepts from compressed sensing [10, 5] of matrices to and dynamic systems. Let us start with the matrix case of classical compressed sensing:

For a given matrix  $A \in \mathbb{R}^{P \times N}$ ,  $M \gg P$ , and given  $\mathbf{y} \in \mathbb{R}^P$ , solve

$$A\mathbf{x} = \mathbf{y} \quad (38)$$

for  $\mathbf{x}$ . We will refer to this as the *static problem*. In contrast to that we consider the problem: For a given input-output map  $\Phi: \mathcal{U} \rightarrow \mathcal{Y}$  where  $\mathcal{U} = \mathcal{U}_1 \oplus \dots \oplus \mathcal{U}_N$  and  $\mathcal{Y} = \mathcal{Y}_1 \oplus \dots \oplus \mathcal{Y}_P$ ,  $\mathcal{U}_i, \mathcal{Y}_j$  function spaces, and given  $\mathbf{y} \in \mathcal{Y}$ , solve

$$\Phi(\mathbf{u}) = \mathbf{y} \quad (39)$$

for  $\mathbf{u}$ . This will be called the *dynamic problem*. In fact, until we make use of the gammoid structure of a dynamic input-output system,  $\mathcal{U}_i$  and  $\mathcal{Y}_j$  can be arbitrary Banach spaces and  $\Phi$  any operator. Despite this more general validity, we will throughout call  $\mathcal{U}$  the input space and  $\mathcal{Y}$  the output space. The *sparse sensing problem*, either static as considered or dynamic, is understood as finding the sparsest solution of the static or dynamic problem, i.e., a solution  $\hat{\mathbf{u}}$  for which most of the components  $\hat{u}_i$  are identically zero. Assume a component, say  $\hat{u}_1$ , has nonzero norm. Then  $\tilde{\mathbf{u}} = (0, \hat{u}_2, \dots, \hat{u}_L)$  can be considered a compression of  $\hat{\mathbf{u}}$ , since  $\tilde{\mathbf{u}}$  is sparser than  $\hat{\mathbf{u}}$ . If we now find, that the compressed vector yields

$$\|\Phi(\tilde{\mathbf{u}}) - \mathbf{y}\| < \epsilon \quad (40)$$

for some given  $\epsilon$ , that is, if it reproduces the desired output with sufficient accuracy, we call it a solution of the *compressed sensing problem*. The static sparse and compressed sensing problem have been developed into various directions, see for example [46] and [16] which both are good compilations of the field and from where we borrow some notations. A crucial step towards a dynamic compressed sensing will be to define appropriate norms on the spaces  $\mathcal{U}$  and  $\mathcal{Y}$ .

### Input Space

Henceforth we will assume the input component  $u_i \in \mathcal{U}_i$  to lie in  $L^p([0, T])$  for a fixed  $p$  and be piecewise  $C^\infty[0, T]$ .

### Underline Notation

We first introduce the underline notation

$$\underline{u}_i := \|u_i\|_{L^p} \quad (41)$$

and for the whole vector  $\mathbf{u} \in \mathcal{U}$  we write

$$\underline{\mathbf{u}} := \begin{pmatrix} \underline{u_1} \\ \vdots \\ \underline{u_L} \end{pmatrix}, \quad (42)$$

so the underline operator maps  $\mathbf{u}$  to a vector  $\underline{\mathbf{u}} \in \mathbb{R}^N$ . In the more general setting,  $\mathcal{U}_i$  is only assumed to be a Banach space with some norm  $\|\cdot\|_{\mathcal{U}_i}$  and the underline maps according to this norm. The underline notation will help clarify our understanding of sparsity and will be useful for the formulation of theorems and proofs. As the underline is basically a norm, it inherits the properties of a norm. The following lemma merely represent calculation rules for underlined vectors.

LEMMA 15: 1. For  $u_i \in \mathcal{U}_i$  we find  $\underline{u_i} = 0 \Leftrightarrow u_i(t) = 0$  a.e. in  $[0, T]$ .

2. For  $u_i, v_i \in \mathcal{U}_i$  we find  $\underline{u_i + v_i} \leq \underline{u_i} + \underline{v_i}$ .

3. For  $u_i \in \mathcal{U}_i$  and  $a \in \mathbb{R}$  we find  $\underline{au_i} = |a|\underline{u_i}$ .

*Proof.* 1. From the definition of the  $L^p$  spaces we get

$$\|u_i\|_{L^p} = 0 \Leftrightarrow u_i = 0 \text{ a.e.} \quad (43)$$

2. Again from the definition we find

$$\underline{u_i + v_i} = \|u_i + v_i\|_{L^p} \leq \|u_i\|_{L^p} + \|v_i\|_{L^p} = \underline{u_i} + \underline{v_i}. \quad (44)$$

3. Since the  $L^p$ -norm is homogeneous we have

$$\underline{au_i} = \|au_i\|_{L^p} = |a|\|u_i\|_{L^p} = |a|\underline{u_i}. \quad (45)$$

□

### Proper Norm for Inputs

Utilizing the underline notation, we are ready to define the  $q$ -norm on  $\mathcal{U}$  as

$$\|\mathbf{u}\|_q := \|\underline{\mathbf{u}}\|_q \quad (46)$$

where on the right hand side the standard  $q$ -norm on  $\mathbb{R}^L$  is understood.

PROPOSITION 16: *The  $q$ -norm on  $\mathcal{U}$  is a proper norm.*

*Proof.* The  $L^p$  norm and the  $q$ -norm on  $\mathbb{R}^N$  both are proper norms that fulfil the three properties *positive definiteness*, the *triangle property*, and *homogeneity*. Since the  $q$ -norm on  $\mathcal{U}$  is a combination of these two norms, it becomes clear, that it again fulfils these properties.

1. Positive definiteness. We find

$$\|\mathbf{u}\|_q = \|\underline{\mathbf{u}}\|_q \geq 0 \quad (47)$$

where the inequality comes from the fact, that we have a proper norm on  $\mathbb{R}^L$ . Equality holds if and only if  $\underline{\mathbf{u}} = 0$ . Due to lemma 15 this is the case if and only if  $\mathbf{u} = 0$ .

2. Triangle inequality. Let  $\mathbf{u}, \mathbf{v} \in \mathcal{U}$ .

$$\|\mathbf{u} + \mathbf{v}\|_q = \|\underline{\mathbf{u} + \mathbf{v}}\|_q = \left( \sum_{i=1}^N (\underline{u_i + v_i})^q \right)^{1/q} \quad (48)$$

From lemma 15 one can see, that

$$(\underline{u_i + v_i})^q \leq (\underline{u_i} + \underline{v_i})^q \quad (49)$$

so we get

$$\|\mathbf{u} + \mathbf{v}\|_q \leq \left( \sum_{i=1}^N (\underline{u_i} + \underline{v_i})^q \right)^{1/q} = \|\underline{\mathbf{u}} + \underline{\mathbf{v}}\|_q \quad (50)$$

and since the latter is a proper  $q$ -norm on  $\mathbb{R}^L$

$$\|\mathbf{u} + \mathbf{v}\|_q \leq \|\underline{\mathbf{u}}\|_q + \|\underline{\mathbf{v}}\|_q = \|\mathbf{u}\|_q + \|\mathbf{v}\|_q. \quad (51)$$

3. Finally we proof homogeneity. Let  $\mathbf{u} \in \mathcal{U}$  and  $a \in \mathbb{R}$ .

$$\|a\mathbf{u}\|_q = \|\underline{a\mathbf{u}}\|_q = \left( \sum_{i=1}^L (\underline{au_i})^q \right)^{1/q} = \left( \sum_{i=1}^L (|a|\underline{u_i})^q \right)^{1/q} = |a| \left( \sum_{i=1}^L (\underline{u_i})^q \right)^{1/q} = |a| \|\underline{\mathbf{u}}\|_q = |a| \|\mathbf{u}\|_q \quad (52)$$

□

For  $q = 0$  one derives a situation comparable to the “0-norm” on  $\mathbb{R}^L$ . First,

$$\|\mathbf{u}\|_0 := \|\underline{\mathbf{u}}\|_0 \quad (53)$$

counts the non-zero components of  $\underline{\mathbf{u}}$ . Due to lemma 15, a component of  $\underline{\mathbf{u}}$  is zero if and only if the corresponding component of  $\mathbf{u}$  is zero, so  $\|\mathbf{u}\|_0$  is indeed a “0-norm” on  $\mathcal{U}$ .



### Support of an Input

Similar to [46], for an index set  $\Lambda \subseteq \{1, \dots, N\}$  we write  $\mathbf{u}_\Lambda$  for the vector

$$(\mathbf{u}_\Lambda)_i = \begin{cases} u_i & \text{if } i \in \Lambda \\ 0 & \text{if } i \notin \Lambda \end{cases} \quad (54)$$

and with  $\Lambda^c$  we denote the complement in  $\{1, \dots, N\}$ . As in [16] we call  $\Lambda$  the *support* of  $\mathbf{u}$ , if  $\Lambda$  is of minimal cardinality and  $\mathbf{u}_\Lambda = \mathbf{u}$ . Let the index set  $\Lambda$  be given, then

$$\mathcal{U}_\Lambda := \{\mathbf{u} \in \mathcal{U} \mid \text{supp } \mathbf{u} \subseteq \Lambda\} \quad (55)$$

is understood as a restriction of the input space.

If the operator  $\Phi$  is linear, then it can be written as a matrix with components  $\Phi_{ji} : \mathcal{U}_i \rightarrow \mathcal{Y}_j$ . The restriction of the domain

$$\Phi : \mathcal{U}_\Lambda \rightarrow \mathcal{Y} \quad (56)$$

is then equivalent to deleting the columns of  $\Phi$  with index not included in  $\Lambda = (\lambda_1, \dots, \lambda_M)$ . We can also interpret it as a new operator  $\Phi_\Lambda$  with unrestricted domain,

$$\Phi_\Lambda : \mathcal{U}_{\lambda_1} \oplus \dots \oplus \mathcal{U}_{\lambda_M} \rightarrow \mathcal{Y}. \quad (57)$$

If  $\mathcal{U} = \mathbb{R}^L$  and  $\mathcal{Y} = \mathbb{R}^P$ , then  $\Phi_\Lambda$  is simply a  $\mathbb{R}^{P \times M}$  matrix. This case coincides with the static problem and was first considered in [9]. We will make use of the following notation from [46].

The “0-norm” can also be expressed via the support,

$$\text{card supp } \mathbf{u} = \|\mathbf{u}\|_0. \quad (58)$$

The set of  $k$ -sparse inputs is understood as

$$\Sigma_k := \{\mathbf{u} \in \mathcal{U} \mid \|\mathbf{u}\|_0 \leq k\}. \quad (59)$$

One will see, that  $\Sigma_k$  is the union of all  $\mathcal{U}_\Lambda$  with  $\text{card } \Lambda \leq k$ .

The three following facts can be proven directly: Let  $\Lambda_0$  and  $\Lambda_1$  be two index sets with  $\text{card } \Lambda_0 = \text{card } \Lambda_1 = k$  and let  $\mathbf{u} \in \mathcal{U}$ . We find

$$\mathbf{u}_{\Lambda_0}, \mathbf{u}_{\Lambda_1} \in \Sigma_k \quad (60)$$

and

$$\mathbf{u}_{\Lambda_0} + \mathbf{u}_{\Lambda_1} \in \Sigma_{2k}. \quad (61)$$

If  $\Lambda_0$  and  $\Lambda_1$  are disjoint we also get

$$\mathbf{u}_{\Lambda_0} + \mathbf{u}_{\Lambda_1} = \mathbf{u}_{\Lambda_0 \cup \Lambda_1}. \quad (62)$$

LEMMA 17: Let  $\mathbf{u}, \mathbf{v} \in \mathcal{U}$  with disjoint support, then

$$\underline{\mathbf{u}} \pm \underline{\mathbf{v}} = \underline{\mathbf{u}} + \underline{\mathbf{v}} \quad (63)$$

and for the  $q$ -norm

$$\|\underline{\mathbf{u}} - \underline{\mathbf{v}}\|_q = \|\underline{\mathbf{u}} \pm \underline{\mathbf{v}}\|_q = \|\underline{\mathbf{u}} + \underline{\mathbf{v}}\|_q \quad (64)$$

*Proof.* If  $i$  is in the support of  $\mathbf{u}$ , then  $v_i = 0$  and equation (63) reduces to

$$\underline{u}_i = \underline{u}_i \quad (65)$$

which is true. If  $i$  is in the support of  $\mathbf{v}$ , then  $u_i = 0$ . Equation (63) together with lemma 15 then becomes

$$\pm v_i = |\pm 1| v_i = \underline{v}_i \quad (66)$$

which also holds true. If  $i$  is in neither support, the equation becomes trivial.

For equation (66) note, that

$$\|\underline{\mathbf{u}} \pm \underline{\mathbf{v}}\|_q = \|\underline{\mathbf{u}} \pm \underline{\mathbf{v}}\|_q = \|\underline{\mathbf{u}} + \underline{\mathbf{v}}\|_q \quad (67)$$

where the first equality is clear by definition and the second equality was just proven.

It remains to show, that for any two vectors  $\mathbf{x}, \mathbf{y} \in \mathbb{R}^N$  with disjoint support one gets

$$\|\mathbf{x} - \mathbf{y}\|_q = \|\mathbf{x} + \mathbf{y}\|_q. \quad (68)$$

However due to the disjoint support  $|x_i + y_i|^q = |x_i|^q + |y_i|^q = |x_i - y_i|^q$  since at least one of the two terms is zero. One finds

$$\|\mathbf{x} - \mathbf{y}\|_q^q = \sum_{i=1}^N |x_i - y_i|^q = \sum_{i=1}^N |x_i + y_i|^q = \|\mathbf{x} + \mathbf{y}\|_q^q. \quad (69)$$

□

The following proposition for the case, where  $\mathbf{u}, \mathbf{v}$  are  $\mathbb{R}^N$  vectors, stems from [2] and has already been used for the static problem in [9]. We proof its validity for  $\mathbf{u}, \mathbf{v}$  being input vectors of a dynamic system.

PROPOSITION 18: Let  $\mathbf{u}, \mathbf{v} \in \mathcal{U}$  with disjoint support, then

$$\|\mathbf{u} + \mathbf{v}\|_q^q = \|\mathbf{u}\|_q^q + \|\mathbf{v}\|_q^q. \quad (70)$$

*Proof.* With lemma 17 we find

$$\|\mathbf{u} + \mathbf{v}\|_q^q = \|\underline{\mathbf{u}} + \underline{\mathbf{v}}\|_q^q = \|\underline{\mathbf{u}} + \underline{\mathbf{v}}\|_q^q = \sum_{i=1}^N (\underline{u}_i + \underline{v}_i)^q. \quad (71)$$

Again due to the disjoint support we can write

$$(\underline{u}_i + \underline{v}_i)^q = (\underline{u}_i)^q + (\underline{v}_i)^q \quad (72)$$

to get

$$\|\mathbf{u} + \mathbf{v}\|_q^q = \sum_{i=1}^N (\underline{u}_i)^q + \sum_{i=1}^N (\underline{v}_i)^q = \|\mathbf{u}\|_q^q + \|\mathbf{v}\|_q^q. \quad (73)$$

□

We close the investigation of the input space with three lemmas on norm-inequalities. For  $\mathbf{u}$  being a  $\mathbb{R}^N$  vector, these lemmas are proven in [46]. For our purposes, it is necessary to prove the validity for the  $q$ -norms on composite Banach spaces.

LEMMA 19: For  $\mathbf{u} \in \Sigma_k$  we find

$$\frac{1}{\sqrt{k}} \|\mathbf{u}\|_1 \leq \|\mathbf{u}\|_2 \leq \sqrt{k} \|\mathbf{u}\|_\infty. \quad (74)$$

*Proof.* Let  $\langle \cdot, \cdot \rangle$  denote the standard scalar product on  $\mathbb{R}^N$ . We can write

$$\|\mathbf{u}\|_1 = \|\underline{\mathbf{u}}\|_1 = \langle \underline{\mathbf{u}}, \text{sgn } \underline{\mathbf{u}} \rangle \leq \|\underline{\mathbf{u}}\|_2 \|\text{sgn } \underline{\mathbf{u}}\|_2, \quad (75)$$

where the latter inequality comes from Cauchy-Schwartz and the signum function is understood component-wise. By assumption  $\mathbf{u}$  is  $k$ -sparse, hence  $\|\text{sgn } \underline{\mathbf{u}}\|_2^2$  is a sum of at most  $k$  ones. We obtain

$$\|\mathbf{u}\|_1 \leq \sqrt{k} \|\underline{\mathbf{u}}\|_2 = \sqrt{k} \|\mathbf{u}\|_2. \quad (76)$$

One will see, that

$$\underline{u}_i \leq \|\underline{\mathbf{u}}\|_\infty = \|\mathbf{u}\|_\infty, \quad (77)$$

where both sides of the inequality are non-negative. Let  $\Lambda = \text{supp } \mathbf{u}$ , then

$$\|\mathbf{u}\|_2^2 = \|\underline{\mathbf{u}}\|_2^2 = \sum_{i \in \Lambda} (\underline{u}_i)^2 \leq \|\mathbf{u}\|_\infty^2 \sum_{i \in \Lambda} 1 = k \|\mathbf{u}\|_\infty^2. \quad (78)$$

Taking the square-root leads to the desired inequality. □

LEMMA 20: For  $\mathbf{u}, \mathbf{v} \in \mathcal{U}$  with disjoint support we find

$$\|\mathbf{u}\|_2 + \|\mathbf{v}\|_2 \leq \sqrt{2}\|\mathbf{u} + \mathbf{v}\|_2. \quad (79)$$

*Proof.* Consider the  $\mathbb{R}^2$  vector

$$\mathbf{x} := \begin{pmatrix} \|\mathbf{u}\|_2 \\ \|\mathbf{v}\|_2 \end{pmatrix}. \quad (80)$$

Lemma 19 holds also for constant vectors and by construction  $\mathbf{x}$  is  $k = 2$  sparse, thus

$$\|\mathbf{x}\|_1 \leq \sqrt{2}\|\mathbf{x}\|_2. \quad (81)$$

We can now replace

$$\|\mathbf{x}\|_1 = \|\mathbf{u}\|_2 + \|\mathbf{v}\|_2. \quad (82)$$

For the right hand side we find

$$\|\mathbf{x}\|_2^2 = \|\mathbf{u}\|_2^2 + \|\mathbf{v}\|_2^2 = \|\mathbf{u} + \mathbf{v}\|_2^2 \quad (83)$$

where the second equality comes from proposition 18. Combining the latter the equations leads to the desired inequality.  $\square$

LEMMA 21: Let  $\mathbf{u} \in \mathcal{U}$  an  $\Lambda_0$  and index set of cardinality  $k$ . For better readability we write  $\mathbf{x} := \mathbf{u}_{\Lambda_0^c}$ . Note, that  $\mathbf{x}$  is a  $\mathbb{R}^N$  vector with non-negative components. Let  $L = (l_1, \dots, l_N)$  a list of indices with  $l_i \neq l_j$  for  $i \neq j$  such that for the components of  $\mathbf{x}$  we find

$$x_{l_1} \geq x_{l_2} \geq \dots \geq x_{l_N}. \quad (84)$$

Define index sets  $\Lambda_1 := \{l_1, \dots, l_k\}$ ,  $\Lambda_2 := \{l_{k+1}, \dots, l_{2k}\}$  and so forth until the whole list  $L$  is covered. If  $k$  is not a divisor of  $N$  the last index set would have less than  $k$  elements. This can be fixed by appending  $\mathbf{u}$  by zero elements.

We find

$$\sum_{j \geq 2} \|\mathbf{u}_{\Lambda_j}\|_2 \leq \frac{\|\mathbf{u}_{\Lambda_0^c}\|_1}{\sqrt{k}} \quad (85)$$

*Proof.* First note, that by construction all  $\Lambda_i$  for  $i = 0, 1, \dots$  are pair-wise disjoint and that

$$\Lambda_0^c = \Lambda_1 \dot{\cup} \Lambda_2 \dot{\cup} \dots \quad (86)$$

For any  $m \in \Lambda_{j-1}$  we get by construction

$$\underline{u}_m \geq \|\mathbf{u}_{\Lambda_j}\|_\infty. \quad (87)$$

We now take the sum over all  $m \in \Lambda_{j-1}$

$$\|\mathbf{u}_{\Lambda_{j-1}}\|_1 \geq k \|\mathbf{u}_{\Lambda_j}\|_\infty. \quad (88)$$

From lemma 19 we have for each  $j$

$$\|\mathbf{u}_{\Lambda_j}\|_2 \leq \sqrt{k} \|\mathbf{u}_{\Lambda_j}\|_\infty \quad (89)$$

and in combination with the latter inequality

$$\|\mathbf{u}_{\Lambda_j}\|_2 \leq \frac{1}{\sqrt{k}} \|\mathbf{u}_{\Lambda_{j-1}}\|_1. \quad (90)$$

We take the sum over  $j \geq 2$

$$\sum_{j \geq 2} \|\mathbf{u}_{\Lambda_j}\|_2 \leq \sum_{j \geq 2} \frac{1}{\sqrt{k}} \|\mathbf{u}_{\Lambda_{j-1}}\|_1. \quad (91)$$

In the right hand side we first perform an index shift and then use proposition 18 to see that

$$\sum_{j \geq 2} \|\mathbf{u}_{\Lambda_{j-1}}\|_1 = \sum_{j \geq 1} \|\mathbf{u}_{\Lambda_j}\|_1 = \|\mathbf{u}_{\Lambda_1 \cup \Lambda_2 \cup \dots}\|_1 = \|\mathbf{u}_{\Lambda_0^c}\|_1. \quad (92)$$

□

## Output Space

### Underline Notation

In analogy to the input space  $\mathcal{U}$ , the underline notation can be used for the output space  $\mathcal{Y} = \mathcal{Y}_1 \oplus \dots \oplus \mathcal{Y}_p$ ,

$$\underline{y}_i := \|y_i\|_{p'}. \quad (93)$$

Here, we assume that each  $y_i \in \mathcal{Y}_i$  is in  $L^{p'}[0, T]$  an piecewise  $C^\infty[0, T]$ . Principally,  $p'$  does not have to match the parameter  $p$  from the input spaces. It will be suppressed from our notation as the result are valid for any fixed value of  $p'$ . Again it would also be sufficient that  $\mathcal{Y}_i$  is a Banach space. The  $q$ -norm on  $\mathcal{Y}$  is defined

$$\|\underline{\mathbf{y}}\|_q := \|\mathbf{y}\|_q. \quad (94)$$

Clearly, all rules we have derived for underlined input vectors hold true for underlined output vectors.

The following lemma yields a last inequality for underlined vectors.

LEMMA 22: Let  $\mathbf{y}, \mathbf{z} \in \mathcal{Y}$ , then

$$\|\underline{\mathbf{y}} - \underline{\mathbf{z}}\|_2^2 \leq \|\mathbf{y} + \mathbf{z}\|_2^2. \quad (95)$$

*Proof.* The inequality can be written as

$$\sum_{i=1}^P (\underline{y}_i - \underline{z}_i)^2 \leq \sum_{i=1}^P (\underline{y}_i + \underline{z}_i)^2. \quad (96)$$

To prove the validity of the latter inequality it suffices to show that

$$|\underline{y}_i - \underline{z}_i| \leq |\underline{y}_i + \underline{z}_i| \quad (97)$$

for each  $i$  in order to complete the proof. First, consider the case  $\underline{y}_i \geq \underline{z}_i$ . From lemma 15 we get

$$\underline{y}_i = (\underline{y}_i + \underline{z}_i) - \underline{z}_i \leq \underline{y}_i + \underline{z}_i + \underline{z}_i \quad (98)$$

and subtracting  $\underline{z}_i$  on both sides yields

$$\underline{y}_i - \underline{z}_i \leq \underline{y}_i + \underline{z}_i. \quad (99)$$

Both sides are positive so (97) holds. Second, consider the case  $\underline{z}_i \geq \underline{y}_i$  and perform the same steps with  $\underline{z}_i$  and  $\underline{y}_i$  swapped to get

$$\underline{z}_i - \underline{y}_i \leq \underline{z}_i + \underline{y}_i. \quad (100)$$

For the right hand side it is clear that

$$\underline{z}_i + \underline{y}_i = \underline{y}_i + \underline{z}_i \quad (101)$$

and for the left hand side

$$\underline{z}_i - \underline{y}_i = |\underline{y}_i - \underline{z}_i| \quad (102)$$

thus equation (97) holds also in this case.  $\square$

## B A Note on the Gammoid of a Dynamic Input-Output System

### Input Sets

The name invertibility can be traced back to the historical development of the subject. Mathematically, a system is invertible if the input-output map

$$\Phi : \mathcal{U} \rightarrow \mathcal{Y} \quad (103)$$

is one-to-one.

We have already introduced the restricted problem

$$\Phi : \mathcal{U}_S \rightarrow \mathcal{Y} \quad (104)$$

where we only allow input vectors  $\mathbf{u}$  whose support lies in  $S \subseteq \{1, \dots, N\}$ .

For the graphical interpretation, we understand  $S$  as the *input set*.

For a given input set  $S$ , one will now see that the operator  $\Phi$  might be one-to-one for the restricted problem (104) while for the unrestricted problem (103) it is not.

## Influence Graph and Structural Invertibility

The definition of the influence graph  $g = (\mathcal{N}, \mathcal{E})$  of a dynamic system is given in the main text. By construction, an input set  $S \subseteq \mathcal{N}$  can be interpreted as a set of nodes in the influence graph. Such a node is also called an *input node*.

The observables of an input-output system are given by a map  $\mathbf{c} : \mathbf{x} \mapsto \mathbf{y}$ ,

$$\mathbf{y}(t) = \mathbf{c}(\mathbf{x}(t)). \quad (105)$$

If, for instance,  $c_1(\mathbf{x}) = x_k$ , then  $y_1 = x_k$  and we can interpret the node  $k \in \mathcal{N}$  as *output node*. Indeed, it is without loss of generality in both, the linear and the non-linear case, that each output component corresponds to one state component. Hence, we get an *out set*  $Z = \{z_1, \dots, z_p\} \subseteq \mathcal{N}$  that characterizes the observables of a system from the graph theoretical point of view.

## Sufficiency of Structural Invertibility

The structural invertibility of a dynamic input-output system is now completely determined by the triplet  $(S, g, Z)$ , as the system is structurally invertible if and only if  $S$  is linked in  $g$  into  $Z$ . It has been shown [43], that structural invertibility of the influence graph is necessary for the invertibility of a system.

To the best of our knowledge, the sufficiency of structural invertibility for the invertibility of a system is an open question. However, we have found the intermediate result:

Say we have an dynamic system with input-output map  $\Phi : \mathcal{U}_S \rightarrow \mathcal{Y}$  where the outputs are characterized by the output set

$$Z = (z_1, \dots, z_p). \quad (106)$$

Assume this system is invertible. Necessarily, the triplet  $(S, g, Z)$  is structurally invertible, where  $g = (\mathcal{N}, \mathcal{E})$  is the influence graph of the system. Now assume, there is a distinct set

$$\tilde{Z} = (\tilde{z}_1, \dots, \tilde{z}_p) \quad (107)$$

with either  $\tilde{z}_i = z_i$  or  $(z_i \rightarrow \tilde{z}_i) \in \mathcal{E}$ . Note, that the output signals from  $Z$  carry enough information to infer the unknown inputs of the system. As each  $\tilde{z}_i$  is either equal or directly influenced by  $z_i$ , it is plausible, that this information is directly passed from  $Z$  to  $\tilde{Z}$ . Unless, we encounter a pathological situation where information is lost in this step.

To give an example for such a pathological situation is given for instance in the toy system

$$\begin{aligned}\dot{x}_1(t) &= x_2(t) \\ \dot{x}_2(t) &= -x_1(t) \\ \dot{x}_3(t) &= x_1(t)x_2(t) \\ \dot{x}_4(t) &= \frac{x_2^2(t) - x_1^2(t)}{x_3(t)}.\end{aligned}\tag{108}$$

We find the differential equation

$$\frac{d}{dt}f + x_3g = 0\tag{109}$$

is solved by the right hand sides  $f = x_1x_2$  and  $g = x_2^2 - x_1^2/x_3$ . Say the functions  $x_1$  and  $x_2$  yield *independent information*. The information content from  $x_3$  and  $x_4$  is not independent any more, but coupled through the differential equation above.

## Gammoid Structure

Consider the triplet  $(S, g, Z)$  with graph  $g = (\mathcal{N}, \mathcal{E})$  and input and output sets  $S, Z \subseteq \mathcal{N}$ . The size of  $S$  and  $Z$  be  $\text{card } S = M$  and  $\text{card } Z = P$ . For a path

$$\pi = (n_0 \rightarrow \dots \rightarrow n_k)\tag{110}$$

with  $n_i \in \mathcal{N}$  and  $(n_i \rightarrow n_{i+1}) \in \mathcal{E}$  we call  $\text{ini}(\pi) = n_0$  the initial node and  $\text{ter}(\pi) = n_k$  the terminal node. For a set  $\Pi$  of paths  $\text{ini } \Pi$  and  $\text{ter } \Pi$  yield the sets of initial and terminal nodes.

**DEFINITION 23:** We say  $S$  is linked in  $g$  to  $Z$ , if there is a family  $\Pi = (\pi_1, \dots, \pi_M)$  of pairwise node-disjoint paths with  $\text{ini}(\Pi) = S$  and  $\text{ter}(\Pi) = Z$ .

The set  $S$  is linked in  $g$  into  $Z$ , if  $\text{ini}(\Pi) = S$  and  $\text{ter}(\Pi) \subseteq Z$ .

The gammoid of a dynamic system assembles all triples  $(S, g, Z)$  into one structure.

First, consider the union of all allowed input nodes  $\mathcal{L}$ . This set is called the *input ground set* and the input sets are understood as the subsets  $S \subseteq \mathcal{L}$ . Without any prior knowledge,  $\mathcal{L} = \mathcal{N}$  is often appropriate.



Second, let  $\mathcal{M}$  be the *output ground set*, i.e., the set of all allowed output nodes. The output set  $Z \subseteq \mathcal{M}$  is understood. Usually, the observables of a dynamic system are given by

$$\mathbf{y}(t) = \mathbf{c}(\mathbf{x}(t)) \quad (111)$$

so the function  $\mathbf{c}$  already determines the output set  $Z$ . In the main text we therefore focus on the case  $Z = \mathcal{M}$ .

However, if we search for an optimal output set it makes sense to first define the output nodes  $\mathcal{M}$  that are principally allowed, and then, e.g., minimize  $Z \subseteq \mathcal{M}$  under the restriction that the structural invertibility condition is fulfilled.

DEFINITION 24: We call  $\Gamma := (\mathcal{L}, \mathbf{g}, \mathcal{M})$  a gammoid.

Gammoids emerge from the graph theoretical problem of node-disjoint path and have been studied earlier without connection to dynamic systems. In [33] a connection was made between gammoids and independence structures. The probably first usage of the word gammoid stems from [35]. The topic has mainly been developed in [36, 34, 19, 26] and also the connection to matroid theory developed in [44] has been discovered.

DEFINITION 25: We say  $S \subseteq \mathcal{L}$  is independent in  $\Gamma = (\mathcal{L}, \mathbf{g}, \mathcal{M})$  if  $S$  is linked into  $\mathcal{M}$ .

The rank-nullity relation for the gammoid  $\Gamma = (\mathcal{L}, \mathbf{g}, \mathcal{M})$  follows from the general investigation of matroids in [44] and states, that for any  $S \in \mathcal{L}$

$$\text{rank } S + \text{null } S = \text{card } S, \quad (112)$$

where  $\text{rank } S$  is the size of the largest independent subset  $T \subseteq S$ . In the main text, the spark of  $\Gamma$  was defined as the largest integer such that

$$\text{card } S < \text{spark } \Gamma \Rightarrow \text{null } S = 0. \quad (113)$$

The following theorem is known for the spark of a matrix [10]. Utilizing gammoid theory, we are able to proof its validity for non-linear dynamic systems.

THEOREM 26: Consider a dynamic input-output system with input-output map  $\Phi: \mathcal{U} \rightarrow \mathcal{Y}$  and gammoid  $\Gamma$ .

Let  $\mathbf{y} \in \mathcal{Y}$  be given. If an input  $\mathbf{u} \in \mathcal{U}$  solves

$$\Phi(\mathbf{u}) = \mathbf{y} \quad (114)$$

and

$$\|\mathbf{u}\|_0 < \frac{\text{spark } \Gamma}{2}, \quad (115)$$

then for any other solution  $\mathbf{v} \in \mathcal{U}$  we find  $\|\mathbf{v}\|_0 > \|\mathbf{u}\|_0$ .

*Proof.* We first reformulate the theorem as follows: There is at most one solution with “0-norm” smaller than  $\frac{\text{spark}\Gamma}{2}$ .

So assume there are two distinct solutions  $\mathbf{u} \neq \mathbf{v}$  that both have “0-norm” smaller than  $\frac{\text{spark}\Gamma}{2}$ . If we denote  $S := \text{supp } \mathbf{u}$  and  $T := \text{supp } \mathbf{v}$  the assumption says

$$\text{card}(S) < \frac{\text{spark}\Gamma}{2} \quad (116)$$

and

$$\text{card}(T) < \frac{\text{spark}\Gamma}{2}. \quad (117)$$

The union  $Q := S \cup T$  has  $\text{card } Q < \text{spark}\Gamma$  thus by definition of the spark

$$\Phi : \mathcal{U}_Q \rightarrow \mathcal{Y} \quad (118)$$

is invertible. So if there is a  $\mathbf{w} \in \mathcal{U}_Q$  that solves

$$\Phi(\mathbf{w}) = \mathbf{y}, \quad (119)$$

this  $\mathbf{w}$  is unique with respect to  $\mathcal{U}_Q$ . By construction  $\mathcal{U}_S \subseteq \mathcal{U}_Q$ , thus  $\mathbf{u}$  is a solution that lies in  $\mathcal{U}_Q$ . So we know that  $\mathbf{w}$  exists and is necessarily equal to  $\mathbf{u}$ . But also  $\mathcal{U}_T \subseteq \mathcal{U}_Q$  so  $\mathbf{w}$  must also equal  $\mathbf{v}$ . We found  $\mathbf{u} = \mathbf{w} = \mathbf{v}$  which contradicts the assumption.  $\square$

## C Convex Optimization

We provide the proof of theorem 9 from the main text.

*Proof.* We first show, that the constraint set

$$\mathcal{A} := \{\mathbf{u} \in \mathcal{U} \mid \|\Phi(\mathbf{u}) - \mathbf{y}\|_2 \leq \epsilon\} \quad (120)$$

with  $\mathbf{y} \in \mathcal{Y}$  and  $\epsilon > 0$  is convex. Let  $\alpha, \beta > 0$  such that  $\alpha + \beta = 1$ . We have to show that

$$\mathbf{u}, \mathbf{v} \in \mathcal{A} \Rightarrow (\alpha\mathbf{u} + \beta\mathbf{v}) \in \mathcal{A}. \quad (121)$$

Given that  $\Phi$  is linear we can estimate

$$\|\Phi(\alpha\mathbf{u} + \beta\mathbf{v}) - \mathbf{y}\|_2 = \|\alpha\Phi(\mathbf{u}) - \alpha\mathbf{y} + \beta\Phi(\mathbf{v}) - \beta\mathbf{y}\|_2 \quad (122)$$

and with the triangle inequality

$$\|\Phi(\alpha\mathbf{u} + \beta\mathbf{v}) - \mathbf{y}\|_2 \leq \alpha\|\Phi(\mathbf{u}) - \mathbf{y}\|_2 + \beta\|\Phi(\mathbf{v}) - \mathbf{y}\|_2 \leq \alpha\epsilon + \beta\epsilon = \epsilon. \quad (123)$$

Since  $\|\cdot\|_q$  is a proper norm on  $\mathcal{U}$  we again apply the triangle inequality

$$\|\alpha\mathbf{u} + \beta\mathbf{v}\|_1 \leq \alpha\|\mathbf{u}\|_1 + \beta\|\mathbf{v}\|_1 \quad (124)$$

to see that the function we want to minimize is convex.  $\square$

## D Restricted Isometry Property

The Restricted Isometry Property first appeared in [6] and was also considered under the name  $\epsilon$ -isometry in [9]. In the following we will consider linear dynamic system.

DEFINITION 27: *The Restricted Isometry Property of order  $2k$  (RIP $2k$ ) is fulfilled if there is a constant  $\delta_{2k}$  such that for  $\mathbf{u}, \mathbf{v} \in \Sigma_k$  the inequalities*

$$(1 - \delta_{2k})\|\underline{\mathbf{u}} - \underline{\mathbf{v}}\|_2^2 \leq \|\underline{\Phi(\mathbf{u})} - \underline{\Phi(\mathbf{v})}\|_2^2 \quad (125)$$

and

$$\|\underline{\Phi(\mathbf{u})} + \underline{\Phi(\mathbf{v})}\|_2^2 \leq (1 + \delta_{2k})\|\underline{\mathbf{u}} + \underline{\mathbf{v}}\|_2^2 \quad (126)$$

hold.

The following lemma was proven for matrices in [46] and can now be generalized to linear dynamic systems.

LEMMA 28: *Assume RIP $2k$  and let  $\mathbf{u}, \mathbf{v}$  with disjoint support. Then*

$$\langle \underline{\Phi(\mathbf{u})}, \underline{\Phi(\mathbf{v})} \rangle \leq \delta_{2k} \|\mathbf{u}\|_2 \|\mathbf{v}\|_2. \quad (127)$$

*Proof.* First we divide (127) by  $\|\mathbf{u}\|_2 \|\mathbf{v}\|_2$  to get a normalized version of (127)

$$\frac{\langle \underline{\Phi(\mathbf{u})}, \underline{\Phi(\mathbf{v})} \rangle}{\|\mathbf{u}\|_2 \|\mathbf{v}\|_2} = \left\langle \underline{\Phi\left(\frac{\mathbf{u}}{\|\mathbf{u}\|_2}\right)}, \underline{\Phi\left(\frac{\mathbf{v}}{\|\mathbf{v}\|_2}\right)} \right\rangle \leq \delta_{2k} \quad (128)$$

where we used the homogeneity of  $\cdot$  and the linearity of  $\Phi$ . Note, that underlined vectors are simply vectors in  $\mathbb{R}^P$ , hence the scalar product is the standard scalar product. For simplicity of notation we henceforth assume  $\|\mathbf{u}\|_2 = \|\mathbf{v}\|_2 = 1$ . We apply the parallelogram identity to the left hand side of (127) to get

$$\langle \underline{\Phi(\mathbf{u})}, \underline{\Phi(\mathbf{v})} \rangle = \frac{1}{4} (\|\underline{\Phi(\mathbf{u})} + \underline{\Phi(\mathbf{v})}\|_2^2 - \|\underline{\Phi(\mathbf{u})} - \underline{\Phi(\mathbf{v})}\|_2^2) \quad (129)$$

and since RIP $2k$  holds we get

$$\langle \underline{\Phi(\mathbf{u})}, \underline{\Phi(\mathbf{v})} \rangle = \frac{1}{4} ((1 + \delta_{2k})\|\underline{\mathbf{u}} + \underline{\mathbf{v}}\|_2^2 - (1 - \delta_{2k})\|\underline{\mathbf{u}} - \underline{\mathbf{v}}\|_2^2). \quad (130)$$

We apply lemma 17 to see that due to the disjoint support we get

$$\|\underline{\mathbf{u}} + \underline{\mathbf{v}}\|_2^2 = \|\underline{\mathbf{u}} - \underline{\mathbf{v}}\|_2^2 = \|\mathbf{u} + \mathbf{v}\|_2^2 \quad (131)$$

and proposition 18 yields

$$\langle \underline{\Phi(\mathbf{u})}, \underline{\Phi(\mathbf{v})} \rangle \leq 2\delta_{2k} (\|\mathbf{u}\|_2^2 + \|\mathbf{v}\|_2^2) = \delta_{2k}. \quad (132)$$

□

To see that our framework is in agreement with the results for the static problem consider the following: Let  $A \in \mathbb{R}^{P \times N}$  and  $\mathbf{y} \in \mathbb{R}^P$  be given and  $\mathbf{w} \in \mathbb{R}^N$ . Solve

$$A\mathbf{w} = \mathbf{y} \tag{133}$$

for  $\mathbf{w}$ . This problem can be seen as a dynamic system with trivial time-development and input-output map  $A$ . Consequently an input set  $S = \{s_1, s_2, \dots\}$  is independent in the gammoid if and only if the columns  $\{\mathbf{a}_{s_1}, \mathbf{a}_{s_2}, \dots\}$  of  $A$  are linearly independent. In this special case we can drop the underline notation and we can rewrite the RIP2k condition as follows. Let  $\kappa := 2k$ . For each  $\mathbf{u}, \mathbf{v} \in \Sigma_k$

$$(1 - \delta_{2k})\|\mathbf{u} - \mathbf{v}\|_2^2 \leq \|A\mathbf{u} - A\mathbf{v}\|_2^2 \tag{134}$$

is equivalent to saying that for each  $\mathbf{w} := \mathbf{u} - \mathbf{v}$  in  $\Sigma_{2k} = \Sigma_\kappa$  we have

$$(1 - \delta_\kappa)\|\mathbf{w}\|_2^2 \leq \|A\mathbf{w}\|_2^2. \tag{135}$$

The same argumentation holds for the second inequality, so that we can say, the system has the RIP of order  $\kappa$  if and only if for all  $\mathbf{w} \in \Sigma_\kappa$

$$(1 - \delta_\kappa)\|\mathbf{w}\|_2^2 \leq \|A\mathbf{w}\|_2^2 \leq (1 + \delta_\kappa)\|\mathbf{w}\|_2^2. \tag{136}$$

The latter is exactly the RIP condition that one usually formulates for static compressed sensing. We can therefore say, that our framework contains the classical static problem as special case.

We now turn our interest to one important proposition about systems that fulfil the RIP2k. This one corresponds to Lemma 1.3 from [46]. We follow the idea of the proof given there, however, some additional steps are necessary in order to get a result valid for dynamic systems.

**PROPOSITION 29:** *Assume the RIP2k holds and let  $\mathbf{u} \in \mathcal{U}$  and  $k \in \mathbb{N}$ . Let  $\Lambda_0$  be an index set of size  $\text{card} \Lambda_0 \leq k$ . Let  $\Lambda_1$  correspond to the  $k$  largest entries of  $\mathbf{u}_{\Lambda_0^c}$  (see lemma 21),  $\Lambda_2$  to the second largest and so forth. We set  $\Lambda := \Lambda_0 \cup \Lambda_1$  and*

$$\alpha := \frac{\sqrt{2}\delta_{2k}}{1 - \delta_{2k}}, \quad \beta := \frac{1}{1 - \delta_{2k}}. \tag{137}$$

Then

$$\|\mathbf{u}_\Lambda\|_2 \leq \alpha \frac{\|\mathbf{u}_{\Lambda_0^c}\|_1}{\sqrt{k}} + \beta \frac{\langle \Phi(\mathbf{u}_\Lambda), \Phi(\mathbf{u}) \rangle}{\|\mathbf{u}_\Lambda\|_2}. \tag{138}$$

*Proof.* For two complementary sets  $\Lambda$  and  $\Lambda^c$  we have  $\Lambda \cap \Lambda^c = \emptyset$  so that we can use equation (62). Furthermore,  $\Lambda \cup \Lambda^c = \{1, \dots, N\}$  shows that  $\mathbf{u} = \mathbf{u}_\Lambda + \mathbf{u}_{\Lambda^c}$ . Thus due to linearity of  $\Phi$  we get

$$\Phi(\mathbf{u}_\Lambda) = \Phi(\mathbf{u}) - \Phi(\mathbf{u}_{\Lambda^c}). \quad (139)$$

By construction  $\Lambda^c = \Lambda_2 \dot{\cup} \Lambda_3 \dot{\cup} \dots$  so we can substitute the latter term by a sum

$$\Phi(\mathbf{u}_\Lambda) = \Phi(\mathbf{u}) - \sum_{j \geq 2} \Phi(\mathbf{u}_{\Lambda_j}). \quad (140)$$

By construction we also know that  $\mathbf{u}_{\Lambda_0}, \mathbf{u}_{\Lambda_1} \in \Sigma_k$ , so from the RIP $2k$  we get

$$(1 - \delta_{2k}) \|\underline{\mathbf{u}}_{\Lambda_0} - \underline{\mathbf{u}}_{\Lambda_1}\|_2^2 \leq \|\underline{\Phi(\mathbf{u}_{\Lambda_0})} - \underline{\Phi(\mathbf{u}_{\Lambda_1})}\|_2^2 \quad (141)$$

On the left hand side we notice that  $\Lambda_0$  and  $\Lambda_1$  are disjoint so we use lemma 17 to see that

$$\|\underline{\mathbf{u}}_{\Lambda_0} - \underline{\mathbf{u}}_{\Lambda_1}\|_2^2 = \|\mathbf{u}_{\Lambda_0} + \mathbf{u}_{\Lambda_1}\|_2^2 = \|\mathbf{u}_\Lambda\|_2^2. \quad (142)$$

On the right hand side we use lemma 22 and the linearity of  $\Phi$  to get

$$\|\underline{\Phi(\mathbf{u}_{\Lambda_0})} - \underline{\Phi(\mathbf{u}_{\Lambda_1})}\|_2^2 \leq \|\underline{\Phi(\mathbf{u}_{\Lambda_0})} + \underline{\Phi(\mathbf{u}_{\Lambda_1})}\|_2^2 = \|\underline{\Phi(\mathbf{u}_\Lambda)}\|_2^2. \quad (143)$$

We can estimate  $\|\Phi(\mathbf{u}_\Lambda)\|_2^2$  by

$$\|\Phi(\mathbf{u}_\Lambda)\|_2^2 \leq \left\langle \underline{\Phi(\mathbf{u}_\Lambda)}, \underline{\Phi(\mathbf{u})} \right\rangle + \left\langle \underline{\Phi(\mathbf{u}_\Lambda)}, \sum_{j \geq 2} \underline{\Phi(\mathbf{u}_{\Lambda_j})} \right\rangle. \quad (144)$$

To see that, we first wrote the norm as a scalar product

$$\|\Phi(\mathbf{u}_\Lambda)\|_2^2 = \left\langle \underline{\Phi(\mathbf{u}_\Lambda)}, \underline{\Phi(\mathbf{u}) - \sum_{j \geq 2} \Phi(\mathbf{u}_{\Lambda_j})} \right\rangle \quad (145)$$

where the second vector comes from equation (140). The triangle inequality from lemma 15 yields

$$\underline{\Phi(\mathbf{u}) - \sum_{j \geq 2} \Phi(\mathbf{u}_{\Lambda_j})} \leq \underline{\Phi(\mathbf{u})} + \underline{\sum_{j \geq 2} \Phi(\mathbf{u}_{\Lambda_j})} \quad (146)$$

as well as

$$\underline{\sum_{j \geq 2} \Phi(\mathbf{u}_{\Lambda_j})} \leq \underline{\sum_{j \geq 2} \Phi(\mathbf{u}_{\Lambda_j})} \quad (147)$$

for each component  $i = 1, \dots, P$ . We proceed with the second scalar product in equation (144)

$$\left\langle \frac{\Phi(\mathbf{u}_\Lambda)}{\sum_{j \geq 2} \Phi(\mathbf{u}_{\Lambda_j})} \right\rangle = \left\langle \frac{\Phi(\mathbf{u}_{\Lambda_0})}{\sum_{j \geq 2} \Phi(\mathbf{u}_{\Lambda_j})} \right\rangle + \left\langle \frac{\Phi(\mathbf{u}_{\Lambda_1})}{\sum_{j \geq 2} \Phi(\mathbf{u}_{\Lambda_j})} \right\rangle \quad (148)$$

where we again used the linearity and triangle inequality in each component,

$$\underline{\Phi}_i(\mathbf{u}_\Lambda) = \underline{\Phi}_i(\mathbf{u}_{\Lambda_0}) + \underline{\Phi}_i(\mathbf{u}_{\Lambda_1}) \leq \underline{\Phi}_i(\mathbf{u}_{\Lambda_0}) + \underline{\Phi}_i(\mathbf{u}_{\Lambda_1}). \quad (149)$$

For  $m = 0, 1$  we first write the sum outside of the scalar product and apply lemma 28

$$\left\langle \frac{\Phi(\mathbf{u}_{\Lambda_m})}{\sum_{j \geq 2} \Phi(\mathbf{u}_{\Lambda_j})} \right\rangle = \sum_{j \geq 2} \left\langle \frac{\Phi(\mathbf{u}_{\Lambda_m})}{\Phi(\mathbf{u}_{\Lambda_j})} \right\rangle \leq \sum_{j \geq 2} \delta_{2k} \|\mathbf{u}_{\Lambda_m}\|_2 \|\mathbf{u}_{\Lambda_j}\|_2 \quad (150)$$

and then lemma 21 to get

$$\left\langle \frac{\Phi(\mathbf{u}_{\Lambda_m})}{\sum_{j \geq 2} \Phi(\mathbf{u}_{\Lambda_j})} \right\rangle \leq \delta_{2k} \|\mathbf{u}_{\Lambda_m}\|_2 \frac{\|\mathbf{u}_{\Lambda_0^c}\|_1}{\sqrt{k}}. \quad (151)$$

We add the two inequalities for  $m = 0$  and  $m = 1$  to get

$$\left\langle \frac{\Phi(\mathbf{u}_\Lambda)}{\sum_{j \geq 2} \Phi(\mathbf{u}_{\Lambda_j})} \right\rangle \leq \delta_{2k} (\|\mathbf{u}_{\Lambda_0}\|_2 + \|\mathbf{u}_{\Lambda_1}\|_2) \frac{\|\mathbf{u}_{\Lambda_0^c}\|_1}{\sqrt{k}}. \quad (152)$$

From lemma 20 we know that

$$\|\mathbf{u}_{\Lambda_0}\|_2 + \|\mathbf{u}_{\Lambda_1}\|_2 \leq \sqrt{2} \|\mathbf{u}_{\Lambda_0} + \mathbf{u}_{\Lambda_1}\|_2 = \sqrt{2} \|\mathbf{u}_\Lambda\|_2. \quad (153)$$

We combine all these results to get

$$(1 - \delta_{2k}) \|\mathbf{u}_\Lambda\|_2^2 \leq \langle \underline{\Phi}(\mathbf{u}_\Lambda), \underline{\Phi}(\mathbf{u}) \rangle + \delta_{2k} \sqrt{2} \|\mathbf{u}_\Lambda\|_2 \frac{\|\mathbf{u}_{\Lambda_0^c}\|_1}{\sqrt{k}}. \quad (154)$$

For  $\delta_{2k} < 1$  and with  $\alpha$  and  $\beta$  as defined above we can divide the inequality by  $(1 - \delta) \|\mathbf{u}_\Lambda\|_2$  to get the desired inequality

$$\|\mathbf{u}_\Lambda\|_2 \leq \alpha \frac{\|\mathbf{u}_{\Lambda_0^c}\|_1}{\sqrt{k}} + \beta \frac{\langle \underline{\Phi}(\mathbf{u}_\Lambda), \underline{\Phi}(\mathbf{u}) \rangle}{\|\mathbf{u}_\Lambda\|_2}. \quad (155)$$

□

We want to make use of the latter proposition in the following way: Say  $\mathbf{v} \in \mathcal{U}$  is a fixed vector, e.g., the true model error that we want to reconstruct, and  $\mathbf{u}$  is our estimate for the model error, e.g., obtained by some optimization procedure. To measure how good the optimization procedure performs, we compute the difference  $\mathbf{w} := \mathbf{u} - \mathbf{v}$  and utilize the proposition to get an upper bound for  $\|\mathbf{w}\|_2$

Now assume the RIP2k holds with a constant  $\delta_{2k} < \sqrt{2} - 1$ . For the proposition we can choose an arbitrary index set  $\Lambda_0$  of size  $k$ . We choose  $\Lambda_0$  such that it corresponds to the  $k$  components of  $\underline{\mathbf{v}}$  with highest magnitude. As said in the proposition,  $\Lambda_1$  will now correspond to the  $k$  largest components in  $\underline{\mathbf{w}_{\Lambda_0^c}}$ ,  $\Lambda_2$  to the second largest and so forth and we set  $\Lambda = \Lambda_0 \cup \Lambda_1$ .

Recap, that  $\sigma_k(\mathbf{v})_q$  is the distance between  $\mathbf{v}$  and the the best  $k$ -sparse approximation [16]

$$\sigma_k(\mathbf{v})_q := \min_{\tilde{\mathbf{v}} \in \Sigma_k} \|\tilde{\mathbf{v}} - \mathbf{v}\|_q \quad (156)$$

and note that

$$\sigma_k(\mathbf{v})_1 = \|\mathbf{v}_{\Lambda_0} - \mathbf{v}\|_1. \quad (157)$$

To see the latter equation, let  $\tilde{\mathbf{v}} \in \Sigma_k$  such that  $\|\tilde{\mathbf{v}} - \mathbf{v}\|_1$  is minimal. Since  $\tilde{\mathbf{v}}$  is  $k$ -sparse, there is a  $\tilde{\Lambda}$  such that  $\tilde{\mathbf{v}} = \tilde{\mathbf{v}}_{\tilde{\Lambda}}$ . Written as a sum

$$\|\tilde{\mathbf{v}} - \mathbf{v}\|_1 = \sum_{i \in \tilde{\Lambda}} \tilde{v}_i - v_i + \sum_{i \in \tilde{\Lambda}^c} v_i. \quad (158)$$

The non-zero components must be chosen  $\tilde{v}_i = v_i$  since this makes the first sum vanish. In order to minimize the second sum the index set  $\tilde{\Lambda}^c$  must correspond to the smallest  $v_i$ , in other words,  $\tilde{\Lambda}$  corresponds to the largest  $v_i$ , thus  $\tilde{\mathbf{v}} = \mathbf{v}_{\Lambda_0}$ .

In the remainder of this section we follow the argumentation line of [46] where the static problem in  $\mathbb{R}^N$  was considered. Therein, many results are utilized that were first presented in [7]. We show, how a line of reasoning can be made for the general case of composite Banach spaces, i.e., valid for dynamic systems.

LEMMA 30: *Consider the setting explained above and assume  $\|\mathbf{u}\|_1 \leq \|\mathbf{v}\|_1$ . Then*

$$\|\mathbf{w}\|_2 \leq 2\|\mathbf{w}_{\Lambda}\|_2 + 2\frac{\sigma_k(\mathbf{v})_1}{\sqrt{k}}. \quad (159)$$

*Proof.* We begin with splitting  $\mathbf{w}$  and applying the triangle inequality

$$\|\mathbf{w}\|_2 = \|\mathbf{w}_{\Lambda} + \mathbf{w}_{\Lambda^c}\|_2 \leq \|\mathbf{w}_{\Lambda}\|_2 + \|\mathbf{w}_{\Lambda^c}\|_2. \quad (160)$$

Since  $\Lambda^c = \Lambda_2 \dot{\cup} \Lambda_3 \dot{\cup} \dots$  we can apply the triangle inequality and lemma 21

$$\|\mathbf{w}_{\Lambda^c}\|_2 = \left\| \sum_{j \geq 2} \mathbf{w}_{\Lambda_j} \right\|_2 \leq \sum_{j \geq 2} \|\mathbf{w}_{\Lambda_j}\|_2 \leq \frac{\|\mathbf{w}_{\Lambda_0^c}\|_1}{\sqrt{k}}. \quad (161)$$

By construction  $\mathbf{u} = \mathbf{v} + \mathbf{w}$  so it is clear that

$$\|\mathbf{v} + \mathbf{w}\|_1 \leq \|\mathbf{v}\|_1. \quad (162)$$

For the complementary sets  $\Lambda_0$  and  $\Lambda_0^c$  we can apply proposition 18 with  $q = 1$  to get

$$\|\mathbf{v} + \mathbf{w}\|_1 = \|\mathbf{v}_{\Lambda_0} + \mathbf{w}_{\Lambda_0}\|_1 + \|\mathbf{w}_{\Lambda_0^c} + \mathbf{v}_{\Lambda_0^c}\|_1. \quad (163)$$

In the proof of lemma 22 we know for each component that

$$\left| \underline{v}_i - \underline{w}_i \right| \leq \underline{v}_i + \underline{w}_i. \quad (164)$$

So we estimate the norm

$$\begin{aligned} \|\mathbf{v}_{\Lambda_0} + \mathbf{w}_{\Lambda_0}\|_1 &= \sum_{i \in \Lambda_0} \underline{v}_i + \underline{w}_i \geq \sum_{i \in \Lambda_0} \left| \underline{v}_i - \underline{w}_i \right| \\ &\geq \left| \sum_{i \in \Lambda_0} (\underline{v}_i - \underline{w}_i) \right| = |(\|\mathbf{v}_{\Lambda_0}\|_1 - \|\mathbf{w}_{\Lambda_0}\|_1)| \geq \|\mathbf{v}_{\Lambda_0}\|_1 - \|\mathbf{w}_{\Lambda_0}\|_1 \end{aligned} \quad (165)$$

and the same holds for  $\Lambda_0^c$ . With this result equation (163) becomes

$$\|\mathbf{v}_{\Lambda_0}\|_1 - \|\mathbf{w}_{\Lambda_0}\|_1 + \|\mathbf{w}_{\Lambda_0^c}\|_1 - \|\mathbf{v}_{\Lambda_0^c}\|_1 \leq \|\mathbf{v}\|_1 \quad (166)$$

which yields a lower bound for  $\|\mathbf{w}_{\Lambda_0^c}\|_1$

$$\|\mathbf{w}_{\Lambda_0^c}\|_1 \leq \|\mathbf{v}\|_1 - \|\mathbf{v}_{\Lambda_0}\|_1 + \|\mathbf{w}_{\Lambda_0}\|_1 + \|\mathbf{v}_{\Lambda_0^c}\|_1. \quad (167)$$

A calculation as in equation (165) and equation (157) show that

$$\|\mathbf{v}\|_1 - \|\mathbf{v}_{\Lambda_0}\|_1 \leq \|\mathbf{v} - \mathbf{v}_{\Lambda_0}\|_1 = \sigma_k(\mathbf{v})_1 \quad (168)$$

and since  $\Lambda_0^c$  is complementary to  $\Lambda_0$ ,  $\mathbf{v} = \mathbf{v}_{\Lambda_0} + \mathbf{v}_{\Lambda_0^c}$ , thus

$$\|\mathbf{v}_{\Lambda_0^c}\|_1 = \|\mathbf{v} - \mathbf{v}_{\Lambda_0}\|_1 = \sigma_k(\mathbf{v})_1. \quad (169)$$

Combining the latter three results we get

$$\|\mathbf{w}_{\Lambda_0^c}\|_1 \leq \|\mathbf{w}_{\Lambda_0}\|_1 + 2\sigma_k(\mathbf{v})_1. \quad (170)$$



Inserting the latter result into equation (161) yields

$$\|\mathbf{w}_{\Lambda^c}\|_2 \leq \frac{\|\mathbf{w}_{\Lambda_0}\|_1 + 2\sigma_k(\mathbf{v})_1}{\sqrt{k}}. \quad (171)$$

From lemma 19 we get

$$\|\mathbf{w}_{\Lambda^c}\|_2 \leq \|\mathbf{w}_{\Lambda_0}\|_2 + 2\frac{\sigma_k(\mathbf{v})_1}{\sqrt{k}}. \quad (172)$$

We now use the triangle inequality

$$\|\mathbf{w}\|_2 \leq \|\mathbf{w}_{\Lambda}\|_2 + \|\mathbf{w}_{\Lambda^c}\|_2 \quad (173)$$

and the fact, that  $\Lambda_0 \subseteq \Lambda$ , thus

$$\|\mathbf{w}_{\Lambda_0}\|_2 \leq \|\mathbf{w}_{\Lambda}\|_2 \quad (174)$$

to get the desired inequality

$$\|\mathbf{w}\| \leq 2\|\mathbf{w}_{\Lambda}\|_2 + 2\frac{\sigma_k(\mathbf{v})_1}{\sqrt{k}}. \quad (175)$$

□

The following theorem follows from a combination of proposition 29 and lemma 30. It is the key result for the optimization problem we present for linear dynamic input-output systems.

**THEOREM 31:** *Let  $\mathbf{u}, \mathbf{v} \in \mathcal{U}$  with  $\|\mathbf{u}\|_1 \leq \|\mathbf{v}\|_1$  and assume for  $\Phi$  we have the RIP $2k$  with  $\delta_{2k} < \sqrt{2} - 1$ . Let  $\Lambda_0$  correspond to the  $k$  largest components of  $\underline{\mathbf{v}}$ . We set  $\mathbf{w} := \mathbf{u} - \mathbf{v}$  and let  $\Lambda_1$  correspond to the  $k$  largest components of  $\mathbf{w}_{\Lambda_0^c}$ ,  $\Lambda_2$  to the second largest and so forth. Let  $\Lambda := \Lambda_0 \cup \Lambda_1$ . There are two constants  $C_0$  and  $C_1$  such that*

$$\|\mathbf{w}\|_2 \leq C_0 \frac{\sigma_k(\mathbf{v})_1}{\sqrt{k}} + C_1 \frac{\langle \Phi(\mathbf{w}_{\Lambda}), \Phi(\mathbf{w}) \rangle}{\|\mathbf{w}_{\Lambda}\|_2}. \quad (176)$$

*Proof.* We start with proposition 29 applied to  $\mathbf{w}$

$$\|\mathbf{w}_{\Lambda}\|_2 \leq \alpha \frac{\|\mathbf{w}_{\Lambda_0^c}\|_1}{\sqrt{k}} + \beta \frac{\langle \Phi(\mathbf{w}_{\Lambda}), \Phi(\mathbf{w}) \rangle}{\|\mathbf{w}_{\Lambda}\|_2}. \quad (177)$$

In lemma 30 equation 172 we found an estimate of  $\|\mathbf{w}_{\Lambda_0^c}\|_1$ , inserted into the latter inequality

$$\|\mathbf{w}_\Lambda\|_2 \leq \alpha \frac{\|\mathbf{w}_{\Lambda_0}\|_1}{\sqrt{k}} + 2\alpha \frac{\sigma_k(\mathbf{v})_1}{\sqrt{k}} + \beta \frac{\langle \Phi(\mathbf{w}_\Lambda), \Phi(\mathbf{w}) \rangle}{\|\mathbf{w}_\Lambda\|_2}. \quad (178)$$

The first term can be treated with lemma 19 and then we use the fact that  $\Lambda_0 \subseteq \Lambda$ , thus  $\|\mathbf{w}_{\Lambda_0}\|_2 \leq \|\mathbf{w}_\Lambda\|_2$ , to get

$$\|\mathbf{w}_\Lambda\|_2 \leq \alpha \|\mathbf{w}_\Lambda\|_2 + 2\alpha \frac{\sigma_k(\mathbf{v})_1}{\sqrt{k}} + \beta \frac{\langle \Phi(\mathbf{w}_\Lambda), \Phi(\mathbf{w}) \rangle}{\|\mathbf{w}_\Lambda\|_2}. \quad (179)$$

Due to the assumption  $\delta_{2k} < \sqrt{2} - 1$  we also get  $\alpha < \sqrt{2} - 1 < 1$  hence  $(1 - \alpha)$  is positive so we rewrite the latter equation as

$$\|\mathbf{w}_\Lambda\|_2 \leq \frac{2\alpha}{1-\alpha} \frac{\sigma_k(\mathbf{v})_1}{\sqrt{k}} + \frac{\beta}{1-\alpha} \frac{\langle \Phi(\mathbf{w}_\Lambda), \Phi(\mathbf{w}) \rangle}{\|\mathbf{w}_\Lambda\|_2}. \quad (180)$$

To close the proof we use lemma 30 to get

$$\frac{1}{2} \left( \|\mathbf{w}\| - 2 \frac{\sigma_k(\mathbf{v})_1}{\sqrt{k}} \right) \leq \frac{2\alpha}{1-\alpha} \frac{\sigma_k(\mathbf{v})_1}{\sqrt{k}} + \frac{\beta}{1-\alpha} \frac{\langle \Phi(\mathbf{w}_\Lambda), \Phi(\mathbf{w}) \rangle}{\|\mathbf{w}_\Lambda\|_2} \quad (181)$$

and with

$$C_0 := \left( \frac{4\alpha}{1-\alpha} + 2 \right) \quad (182)$$

and

$$C_1 := \frac{2\beta}{1-\alpha} \quad (183)$$

we finally obtain

$$\|\mathbf{w}\|_2 \leq C_0 \frac{\sigma_k(\mathbf{v})_1}{\sqrt{k}} + C_1 \frac{\langle \Phi(\mathbf{w}_\Lambda), \Phi(\mathbf{w}) \rangle}{\|\mathbf{w}_\Lambda\|_2}. \quad (184)$$

□

We can now apply theorem 31 to the solutions of the  $\|\cdot\|_0$  and  $\|\cdot\|_1$  optimization problems. Assume  $\mathbf{y}^{\text{data}} \in \mathcal{Y}$  is given data which is produced by a sparse “true” input  $\mathbf{w}^* \in \mathcal{U}$ , i.e.,

$$\Phi(\mathbf{w}^*) = \mathbf{y}^{\text{data}}. \quad (185)$$

We want to infer  $\mathbf{w}^*$  from  $\mathbf{y}^{\text{data}}$ . Sparsity of the “true” input  $\mathbf{w}^*$  means, that for all  $\mathbf{u}$  in

$$\mathcal{A} := \{\mathbf{u} \in \mathcal{U} \mid \|\Phi(\mathbf{u}) - \mathbf{y}\|_2 = 0\} \quad (186)$$

we find

$$\|\mathbf{w}^*\|_0 \leq \|\mathbf{u}\|_0. \quad (187)$$

Now let  $\hat{\mathbf{w}}$  be a solution of the convex  $\|\cdot\|_1$  optimization problem, that is, for all  $\mathbf{u} \in \mathcal{A}$  we find

$$\|\hat{\mathbf{w}}\|_1 \leq \|\mathbf{u}\|_1. \quad (188)$$

We can now apply theorem 31 to  $\mathbf{w} = \hat{\mathbf{w}} - \mathbf{w}^*$ . Note, that

$$\Phi(\hat{\mathbf{w}}) = \Phi(\mathbf{w}^*) \Rightarrow \Phi(\mathbf{w}) = 0. \quad (189)$$

We find

$$\|\hat{\mathbf{w}} - \mathbf{w}^*\|_2 \leq C_0 \frac{\sigma_k(\mathbf{w}^*)_1}{\sqrt{k}}. \quad (190)$$

Note that by definition  $\sigma_k(\mathbf{w}^*)_1$  is the best  $k$ -sparse approximation to  $\mathbf{w}^*$  in 1-norm. Thus we have shown, that the convex  $\|\cdot\|_1$  optimization yields an approximation of the unknown “true” input.

Theorem 31 might be adjusted for various scenarios where we can make further assumptions about the model error  $\mathbf{w}^*$  or about stochastic or measurement errors. We want to derive a last inequality for the case of bounded noise. Let  $\xi$  represent the noise, and  $\Phi_{\text{noiseless}}$  the solution operator we have discussed so far. We now consider a new solution operator

$$\Phi(\mathbf{u})(t) := \Phi_{\text{noiseless}}(\mathbf{u})(t) + \xi(t) \quad (191)$$

that incorporates the noise  $\xi$ . Since  $\xi(t) \in \mathbb{R}^P$  we can interpret  $\xi \in \mathcal{Y}$  and use the norm on  $\mathcal{Y}$ . We assume that  $\xi$  is a bounded noise with  $\epsilon > 0$ ,

$$\|\xi\|_2 \leq \epsilon. \quad (192)$$

We adjust the solution set

$$\mathcal{A} := \{\mathbf{u} \in \mathcal{U} \mid \|\Phi(\mathbf{u}) - \mathbf{y}\|_2 \leq \epsilon\} \quad (193)$$

and define  $\mathbf{w}^*$ ,  $\hat{\mathbf{w}} \in \mathcal{A}$  as before with minimal  $\|\cdot\|_0$  and  $\|\cdot\|_1$  norm, respectively. From the theorem we get

$$\|\mathbf{w}\|_2 \leq C_0 \frac{\sigma_k(\mathbf{w}^*)_1}{\sqrt{k}} + C_1 \frac{\langle \Phi(\mathbf{w}_\Lambda), \Phi(\mathbf{w}) \rangle}{\|\mathbf{w}_\Lambda\|_2}. \quad (194)$$

We want to estimate the scalar product by the Cauchy-Schwartz inequality

$$\langle \underline{\Phi(\mathbf{w}_\Lambda)}, \underline{\Phi(\mathbf{w})} \rangle \leq \|\Phi(\mathbf{w}_\Lambda)\|_2 \|\Phi(\mathbf{w})\|_2. \quad (195)$$

By construction  $\Lambda = \Lambda_0 \cup \Lambda_1$  has at most  $2k$  elements. thus, it is possible to write  $\mathbf{w} = \mathbf{u} + \mathbf{v}$  where  $\mathbf{u}, \mathbf{v} \in \Sigma_k$  have disjoint support. With lemma 15 we get

$$\|\Phi(\mathbf{w}_\Lambda)\|_2 = \|\underline{\Phi(\mathbf{u}) + \Phi(\mathbf{v})}\|_2 \leq \|\underline{\Phi(\mathbf{u})} + \underline{\Phi(\mathbf{v})}\|_2. \quad (196)$$

We can now use the RIP $2k$  to get

$$\|\Phi(\mathbf{w}_\Lambda)\|_2 \leq \sqrt{1 + \delta_{2k}} \|\underline{\mathbf{u}} + \underline{\mathbf{v}}\|_2 \quad (197)$$

and with lemma 17

$$\|\Phi(\mathbf{w}_\Lambda)\|_2 \leq \sqrt{1 + \delta_{2k}} \|\mathbf{u} + \mathbf{v}\|_2 = \sqrt{1 + \delta_{2k}} \|\mathbf{w}_\Lambda\|_2. \quad (198)$$

On the other hand we can write  $\mathbf{w} = \hat{\mathbf{w}} - \mathbf{w}^*$  and get

$$\|\Phi(\mathbf{w})\| = \|(\Phi(\hat{\mathbf{w}}) - \mathbf{y}) - (\Phi(\mathbf{w}^*) - \mathbf{y})\|_2 \leq \|\Phi(\hat{\mathbf{w}}) - \mathbf{y}\|_2 + \|\Phi(\mathbf{w}^*) - \mathbf{y}\|_2 \leq 2\epsilon. \quad (199)$$

With this, equation (195) becomes

$$\langle \underline{\Phi(\mathbf{w}_\Lambda)}, \underline{\Phi(\mathbf{w})} \rangle \leq 2\epsilon \sqrt{1 + \delta_{2k}} \|\mathbf{w}_\Lambda\|_2 \quad (200)$$

and inserting this into equation (194) leads to

$$\|\mathbf{w}\|_2 \leq C_0 \frac{\sigma_k(\mathbf{w}^*)_1}{\sqrt{k}} + C_1 2\epsilon \sqrt{1 + \delta_{2k}}. \quad (201)$$

We can now adjust the constant  $C_2 := \sqrt{1 + \delta_{2k}} C_1$  to get the result

$$\|\hat{\mathbf{w}} - \mathbf{w}^*\|_2 \leq C_0 \frac{\sigma_k(\mathbf{w}^*)_1}{\sqrt{k}} + C_2 \epsilon \quad (202)$$

which is the equation from theorem 4 of the main text.

## E A Note on Weighted Gammoids

The edge weights of an influence graph are defined by

$$F(i \rightarrow j) := \frac{\partial f_j(\mathbf{x})}{\partial x_i}. \quad (203)$$

Since we only consider linear systems in this section, the edge weights are real valued constants. It is easy to see, that there is a one-to-one correspondence between linear input-output systems and weighted gammoids. However, we want to emphasize, that the construction of the weighted gammoid is not restricted to linear systems, as soon as we allow for state dependent weights, see for instance [43]. The investigation of non-linear gammoids might yield an approach to a non-linear extension of our framework and shall be considered in future research.

From [43] we deduced, that the gammoid of a system contains the information about the structurally invertible input-output configurations. But we also now, that structural properties are not sensitive to numerical ill-posedness. This is the reason why we have examined the possibility of a convex optimization as well as the RIP2k property. Those, however, are hard to verify. Fortunately we can again make use of the gammoid interpretation.

## E.1 Transfer Function

The following lemma is known in the literature (see e.g. [30]), but usually given for adjacency matrices with entries that are either zero or one. We formulate it in a way that is consistent with our notation and such that the edge weights can be arbitrary.

LEMMA 32: *Let  $A \in \mathbb{R}^{N \times N}$  a matrix and  $g = (\mathcal{N}, \mathcal{E})$  the weighted graph with nodes  $\mathcal{N} = \{1, \dots, N\}$  and edges  $(i \rightarrow j) \in \mathcal{E}$  whenever  $A_{ji} \neq 0$ . For each edge we define its weight as  $F(i \rightarrow j) := A_{ji}$ . The edge weights imply a weight for sets of paths. Let  $\mathcal{P}_k(a, b)$  denote the set of paths from node  $a$  to node  $b$  of length  $k$ . Then*

$$A_{ba}^k = F(\mathcal{P}_k(a, b)) \quad (204)$$

*Proof.* Let  $l_0, l_1, \dots, l_k \in \mathcal{N}$  be a list of nodes. If the path  $\pi := (l_0 \rightarrow \dots \rightarrow l_k)$  exists, then  $\pi \in \mathcal{P}_k(l_0, l_k)$  and we can use the homomorphic property of  $F$  to get

$$F(\pi) = F(l_0 \rightarrow l_1) \dots F(l_{k-1} \rightarrow l_k) = A_{l_k l_{k-1}} \dots A_{l_1 l_0}. \quad (205)$$

On the other hand, if  $\pi$  does not exist, that means at least one of the terms  $A_{l_i l_{i-1}}$  equals zero and

$$A_{l_k l_{k-1}} \dots A_{l_1 l_0} = 0. \quad (206)$$

When we compute the powers of  $A$  we find

$$A_{ba}^k = \sum_{l_1, \dots, l_{k-1}=1}^N A_{b l_{k-1}} \dots A_{l_1 a} \quad (207)$$

which sums up all node lists  $l_1, \dots, l_{k-1} \in \mathcal{N}$  with  $l_0 = a$  and  $l_k = b$  fixed. It is clear, that the terms in the sum do not vanish if and only if the path  $(a \rightarrow l_1 \rightarrow \dots \rightarrow l_{k-1} \rightarrow b)$  exists. Thus we can replace the sum by

$$A_{ba}^k = \sum_{\pi \in \mathcal{P}_k(a,b)}^N A_{bl_{k-1}} \dots A_{l_1 a} \quad (208)$$

and we have already seen, that for an existing path we can replace the right hand side by

$$A_{ba}^k = \sum_{\pi \in \mathcal{P}_k(a,b)} F(\pi) = F(\mathcal{P}_k(a,b)) \quad (209)$$

where the second equality comes simply from the definition of the weight function for sets of paths.  $\square$

In Laplace space, a linear dynamic input-output system takes the form

$$\tilde{\mathbf{y}}(\sigma) = T(\sigma) \tilde{\mathbf{w}}(\sigma) \quad (210)$$

where  $\sigma \in \mathbb{C}$  is a complex variable,  $\tilde{\mathbf{w}} : \mathcal{F}$  and  $\tilde{\mathbf{y}}$  are the Laplace transforms of the input  $\mathbf{w}$  and output  $\mathbf{y}$ , respectively, see for instance [24]. One will realize, that the transfer function  $T$  is the Laplace representation of the operator  $\Phi$ .

We have earlier discussed, that for linear systems, an input set  $S$  can either be understood as a restriction to the input space  $\mathcal{U}$ , or, equivalently, as a submatrix of the solution operator  $\Phi$  (in state space) and clearly also  $T$  (in Laplace space). The differential equation of a linear system

$$\dot{\mathbf{x}}(t) = A\mathbf{x}(t) + \mathbf{w}(t) \quad (211)$$

can be written after Laplace transformation as

$$\tilde{\mathbf{x}}(\sigma) = (\sigma - A)^{-1} \tilde{\mathbf{w}}(\sigma). \quad (212)$$

We can interpret

$$T^{\text{full}}(\sigma) = (\sigma - A)^{-1} \quad (213)$$

as the *full transfer function*. For a given input set  $S$  and output set  $Z$  we can then simply take the columns indicated by  $S$  and rows indicated by  $Z$  to get the transfer function for this specific configuration.

**PROPOSITION 33:** *Let  $T^{\text{full}}$  be the full transfer function of a linear system and  $i, j \in \mathcal{N}$  nodes in the weighted influence graph. Let  $\mathcal{P}(i, j)$  denote the paths from  $i$  to  $j$ . Then*

$$T_{ji}^{\text{full}}(\sigma) = \frac{1}{\sigma} \sum_{\pi \in \mathcal{P}(i,j)} \frac{F(\pi)}{\sigma^{\text{len}\pi}}. \quad (214)$$

*Proof.* We use the Neumann-series to write

$$T_{ji}^{\text{full}}(\sigma) = [(\sigma - A)^{-1}]_{ji} = \frac{1}{\sigma} \left[ \left( 1 - \frac{A}{\sigma} \right)^{-1} \right]_{ji} = \frac{1}{\sigma} \sum_{k=0}^{\infty} \frac{[A^k]_{ji}}{\sigma^k}. \quad (215)$$

where the brackets just indicate that we first take the matrix power and then take the  $ji$ -th element. With lemma 32 we get

$$T_{ji}^{\text{full}}(\sigma) = \frac{1}{\sigma} \sum_{k=0}^{\infty} \sum_{\pi \in \mathcal{P}_k(i,j)} \frac{F(\pi)}{\sigma^k}. \quad (216)$$

We now see that in  $\sigma^{-k}$  we always find that  $k$  is the length of the path,  $k = \text{len } \pi$ . Furthermore we can combine the two sums to one sum over all paths

$$T_{ji}^{\text{full}}(\sigma) = \frac{1}{\sigma} \sum_{\pi \in \mathcal{P}(i,j)} \frac{F(\pi)}{\sigma^k}. \quad (217)$$

□

## E.2 Transposed Gammoids

For a linear dynamic system

$$\begin{aligned} \dot{\mathbf{x}}(t) &= A\mathbf{x}(t) + B\mathbf{w}(t) \\ \mathbf{x}(0) &= \mathbf{x}_0 \\ \mathbf{y}(t) &= C\mathbf{x}(t) \end{aligned} \quad (218)$$

the system

$$\begin{aligned} \dot{\mathbf{x}}(t) &= A^T \mathbf{x}(t) + C^T \mathbf{y}(t) \\ \mathbf{x}(0) &= \mathbf{x}_0 \\ \mathbf{w}(t) &= B^T \mathbf{x}(t) \end{aligned} \quad (219)$$

is called *dual* in the literature, referring to the duality principle of optimization theory, see for instance [25]. To avoid confusion, we will use the term *transposed system* instead, which then leads to a *transposed gammoid*. This nomenclature helps avoiding confusion with the term *dual gammoid*, which is already occupied by the duality principle of matroid theory [44] and which, to the best of our knowledge, is not related to dual dynamic systems.

From a gammoid  $\Gamma$  one can easily switch to the transposed gammoid  $\Gamma'$  without detour over the transposed dynamic system. Let  $g$  and  $g'$  denote the influence graphs of the original and the transposed system, respectively. Both

systems have differential equations for the variables  $\mathbf{x} = (x_1, \dots, x_N)^T$ , so both influence graphs have  $N$  nodes. To avoid confusion, say

$$\mathcal{N} = \{1, \dots, N\} \quad (220)$$

and the nodes of the transposed graph are indicated by a prime symbol

$$\mathcal{N}' = \{1', \dots, N'\}. \quad (221)$$

We also have a one-to-one correspondence between the edges  $\mathcal{E}$  and  $\mathcal{E}'$  which can be written as

$$(i \rightarrow j)' = (j' \rightarrow i') \quad (222)$$

which is the gammoid analogue to  $A_{ji} = (A^T)_{ij}$ . This shows, that to switch from  $g$  to  $g'$ , one basically has to flip the edges. Finally, one will realize, that inputs and outputs swap their roles. So if  $S = (s_1, \dots, s_M)$  is an input set in  $g$ , then  $S' = (s'_1, \dots, s'_M)$  is an output set of  $g'$ . In the same way, an output set  $Z$  in  $g$  becomes an input set  $Z'$  in  $g'$ . We find that

$$(\mathcal{L}, g, \mathcal{M})' = (\mathcal{M}', g', \mathcal{L}') \quad (223)$$

directly maps the gammoid  $\Gamma$  to the transposed gammoid  $\Gamma'$ . We have just derived the construction of the transposed gammoid for linear system. Clearly, we can use the derived formula to define the transposed gammoid also for the general case.

DEFINITION 34: *Let  $\Gamma = (\mathcal{L}, g, \mathcal{M})$  be a gammoid, we call*

$$\Gamma' := (\mathcal{M}', g', \mathcal{L}') \quad (224)$$

*the transposed gammoid.*

If the gammoid is a weighted gammoid, one simply keeps the weight of each single edge,

$$F(i \rightarrow j) = F((i \rightarrow j)'). \quad (225)$$

Now any path

$$\pi = (n_0 \rightarrow \dots \rightarrow n_k) \quad (226)$$

in  $\Gamma$  corresponds to a path

$$\pi' = (n'_k \text{ to } \dots \text{ to } n'_0) \quad (227)$$

in  $\Gamma'$  and

$$F(\pi) = F(\pi'). \quad (228)$$



### E.3 Concatenation of Gammoids

Consider two gammoids  $\Gamma_1 = (\mathcal{L}_1, g_1, \mathcal{M}_1)$  and  $\Gamma_2 = (\mathcal{L}_2, g_2, \mathcal{M}_2)$ . If we now think of a signal that flows through a gammoid from the inputs to the outputs we can define the *concatenation*

$$\Gamma := \Gamma_1 \circ \Gamma_2. \quad (229)$$

A signal enters somewhere in the input ground set  $\mathcal{L}_1$  and flows through  $\Gamma_1$  to the output ground set  $\mathcal{M}_1$ . From there, the signal is passed over to  $\mathcal{L}_2$  and flows through  $\Gamma_2$  to the final output ground set  $\mathcal{M}_2$ . To get a well defined concatenation, one must assume, that the signal transfer between the gammoids, i.e., from  $\mathcal{M}_1$  to  $\mathcal{L}_2$  is well defined. To ensure this, we assume, that  $\mathcal{M}_1 = \{m_1, \dots, m_P\}$  and  $\mathcal{L}_2 = \{l_1, \dots, l_P\}$  have the same size and are present in a fixed ordering such that the signal is passed from  $m_i$  to  $l_i$ . In other words, we identify

$$m_i = l_i \quad \text{for } i = 1, \dots, P. \quad (230)$$

The result  $\Gamma = (\mathcal{L}, g, \mathcal{M})$  is indeed again a gammoid with input ground set  $\mathcal{L} = \mathcal{L}_1$  and output ground set  $\mathcal{M} = \mathcal{M}_2$ . The graph  $g$  of this gammoid is simply the union of  $g_1$  and  $g_2$ , i.e.,  $g = (\mathcal{N}_1 \cup \mathcal{N}_2, \mathcal{E}_1 \cup \mathcal{E}_2)$ .

**PROPOSITION 35:** *Let  $\Gamma_1 = (\mathcal{L}_1, g_1, \mathcal{M}_1)$  and  $\Gamma_2 = (\mathcal{L}_2, g_2, \mathcal{M}_2)$  be two gammoids,  $\Gamma = (\mathcal{L}, g, \mathcal{M})$  the result of the concatenation  $\Gamma_1 \circ \Gamma_2$ . For any  $S \subseteq \mathcal{L}$  and  $K \subseteq \mathcal{M}$  we find:  $S$  is linked in  $g$  to  $K$  if and only if there is a  $Z \subseteq \mathcal{M}_1 = \mathcal{L}_2$  such that  $S$  is linked in  $g_1$  to  $Z$  and  $Z$  is linked in  $g_2$  to  $K$ .*

*Proof.* First assume, that  $S \subseteq \mathcal{L}$  is linked in  $g$  to  $K \subseteq \mathcal{M}$  that is, there is a family of node-disjoint paths  $\Pi = \{\pi_1, \dots, \pi_M\}$  from  $S$  to  $\mathcal{M}$ , where  $M = \text{card } S = \text{card } K$ . By construction, for any edge  $i \rightarrow j$  with  $i \in \mathcal{N}_1$  and  $j \in \mathcal{N}_2$  we necessarily find that either  $i \in \mathcal{M}_1$  or  $j \in \mathcal{M}_1$ . Since  $S \subseteq \mathcal{L}_1 \subseteq \mathcal{N}_1$  and  $K \subseteq \mathcal{M}_2 \subseteq \mathcal{N}_2$  it is clear, that each path  $\pi_i$  has at least one node  $z_i \in \mathcal{M}_1$  and these nodes are pairwise distinct. We find that  $Z := \{z_1, \dots, z_M\}$  acts as a separator. We can decompose each path  $\pi_i = \pi_i^1 \circ \pi_i^2$  at  $z_i$  such that  $\pi_i^1$  starts in  $S$  and terminates at  $z_i$  and  $\pi_i^2$  starts at  $z_i$  and terminates in  $K$ . We find that  $\Pi^1 = \{\pi_1^1, \dots, \pi_M^1\}$  is a family of node-disjoint paths such that  $S$  is linked in  $g_1$  to  $Z$ . Analogously through  $\Pi^2$  we see that  $Z$  is linked in  $g_2$  to  $K$ .

Now assume  $S$  is linked in  $g_1$  to  $Z$  and  $Z$  is linked in  $g_2$  to  $K$ . Let  $Z = (z_1, \dots, z_M)$  where again  $M$  is the cardinality of  $S$  and  $K$ . That means we find a set  $\Pi^1 = \{\pi_1^1, \dots, \pi_M^1\}$  of node-disjoint paths such that  $\pi_i^1$  starts in  $S$  and terminates at  $z_i$  and we find a family of node-disjoint paths  $\Pi^2 = \{\pi_1^2, \dots, \pi_M^2\}$  such that  $\pi_i^2$  starts at  $z_i$  and terminates in  $K$ . We can now concatenate the paths

$\pi_i := \pi_i^1 \circ \pi_i^2$ . Since  $\pi_i^1$  only contains nodes from  $\mathcal{N}_1$  and  $\pi_i^2$  from  $\mathcal{N}_2$ , it is clear, that the paths from  $\Pi := \{\pi_1, \dots, \pi_M\}$  are again node-disjoint. Hence  $S$  is linked in  $g$  to  $K$ .  $\square$

A special case is the concatenation of a gammoid with its own transpose,  $\Gamma \circ \Gamma'$ . Due to the symmetry between paths in  $\Gamma$  and  $\Gamma'$  explained before, we find that an input set  $S$  is independent in  $\Gamma \circ \Gamma'$  if and only if it is independent in  $\Gamma$ .

## E.4 Gramian Matrix

DEFINITION 36: Let  $T : \mathbb{C} \rightarrow \mathcal{C}^{P \times M}$  be the transfer function of a linear system. The input gramian of the system is defined as

$$G(\sigma) := T^*(\sigma)T(\sigma) \quad s \in \mathbb{C} \quad (231)$$

where the asterisk denotes hermitian conjugate.

Let  $S = \{s_1, \dots, s_M\}$  be the input set and  $Z = \{z_1, \dots, z_P\}$  be the output set that belongs to the transfer function  $T$ . Making use of proposition 33 we can compute the input gramian via

$$G_{ji}(\sigma) = \sum_{k=1}^P \frac{1}{|\sigma|^2} \sum_{\rho \in \mathcal{P}(s_i, z_k)} \frac{F(\rho)}{\sigma^{\text{len } \rho}} \sum_{\pi \in \mathcal{P}(s_j, z_k)} \frac{F(\pi)}{\bar{\sigma}^{\text{len } \pi}}. \quad (232)$$

We already know that if there is a path  $\pi$  in  $\Gamma$  that goes from  $s_j$  to  $z_k$ , then there is a path  $\pi'$  in  $\Gamma'$  that goes from  $z'_k$  to  $s'_j$ . So if

$$\rho = (n_0 \rightarrow \dots \rightarrow n_{l-1} \rightarrow n_l) \quad (233)$$

is a path in  $\Gamma$  from  $n_0 = s_i$  to  $n_l = z_k$ , and if  $\pi'$

$$\pi' = (p'_0 \rightarrow \dots \rightarrow p'_r) \quad (234)$$

is a path in  $\Gamma'$  from  $p'_0 = z'_k$  to  $p'_r = s'_j$ , then with respect to the identification  $z_k = z'_k$  we can interpret

$$\rho \circ \pi' = (n_0 \rightarrow \dots \rightarrow n_{l-1} \rightarrow p'_0 \rightarrow \dots \rightarrow p'_r) \quad (235)$$

as a path in  $\Gamma \circ \Gamma'$  with

$$F(\rho \circ \pi') = F(\rho)F(\pi') = F(\rho)F(\pi). \quad (236)$$

We can introduce a multi-index notation

$$\sigma^\psi := \sigma^{\text{len } \rho} \bar{\sigma}^{\text{len } \pi} \quad (237)$$

because we know, that any path  $\psi$  in  $\Gamma \circ \Gamma'$  has always a unique decomposition in such a  $\rho$  and  $\pi'$ . We end up with the formula

$$G_{ji}(\sigma) = \frac{1}{|s|^2} \sum_{\psi \in \mathcal{P}(s_i, s'_j)} \frac{F(\psi)}{\sigma^\psi} \quad (238)$$

Before we turn our interest to the meaning of the gramian for dynamic compressed sensing, we want to provide tools in the form of the following lemma and proposition.

LEMMA 37: *Let  $\Gamma = (\mathcal{L}, g, \mathcal{M})$  be a gammoid and let  $a, b \in \mathcal{L}$  be two input nodes. In  $\Gamma \circ \Gamma'$  let  $\eta_{aa'}$  denote the shortest path from  $a$  to  $a'$ ,  $\eta_{bb'}$  the shortest path from  $b$  to  $b'$  and  $\eta_{ab'}$  shall denote the shortest path from  $a$  to  $b'$ . Then*

$$\frac{\text{len}(\eta_{aa'}) + \text{len}(\eta_{bb'})}{2} \leq \text{len}(\eta_{ab'}). \quad (239)$$

*Proof.* By construction we know that there is a  $z \in \mathcal{M}$  and a decomposition  $\eta_{ab'} = \alpha \circ \beta'$  such that  $\alpha$  goes from  $a$  to  $z$  and  $\beta'$  goes from  $b$  to  $z$ . We now find that  $\alpha \circ \alpha'$  goes from  $a$  to  $a'$ . By assumption of the lemma,  $\alpha \circ \alpha'$  is not shorter than  $\eta_{aa'}$ , thus

$$\text{len}(\eta_{aa'}) \leq \text{len}(\alpha \circ \alpha') = 2\text{len}(\alpha). \quad (240)$$

Analogously we find

$$\text{len}(\eta_{bb'}) \leq 2\text{len}(\beta'). \quad (241)$$

We can now add these two inequalities together to get

$$\text{len}(\eta_{aa'}) + \text{len}(\eta_{bb'}) \leq 2(\text{len}(\alpha) + \text{len}(\beta')). \quad (242)$$

On the right hand side we identify the length of  $\eta_{ab'}$  to get

$$\text{len}(\eta_{aa'}) + \text{len}(\eta_{bb'}) \leq 2\text{len}(\eta_{ab'}). \quad (243)$$

□

PROPOSITION 38: *Let  $T$  be the transfer function of a dynamic system with input set  $S = \{s_1, \dots, s_M\}$  and gammoid  $\Gamma$ , and let  $G = T^* T$  be the input gramian. Consider the quantity*

$$\mu_{ij}(\sigma) := \frac{|G_{ij}(\sigma)|}{\sqrt{G_{ii}(\sigma)G_{jj}(\sigma)}}. \quad (244)$$

Let  $\eta_{ij'}$  be the shortest path in  $\Gamma \circ \Gamma$  from  $s_i$  to  $s'_j$ . If lemma 37 holds with equality, then

$$\lim_{|\sigma| \rightarrow \infty} \mu_{ij}(\sigma) = \frac{|F(\eta_{ij'})|}{\sqrt{F(\eta_{ii'})F(\eta_{jj'})}}. \quad (245)$$

If the lemma holds with strict inequality, then

$$\lim_{|\sigma| \rightarrow \infty} \mu_{ij}(\sigma) = 0. \quad (246)$$

Note, that there can be several shortest paths, so  $\eta_{ii'}$  can be a set of paths.

*Proof.* Say  $S = \{s_1, \dots, s_M\}$  is the input set that leads to the transfer function  $T$  and the input gramian  $G$ . Using equation (238) we can write

$$\mu_{ij}(\sigma) = \frac{\left| \sum_{\psi \in \mathcal{P}(s_i, s'_j)} F(\psi) \sigma^{-\psi} \right|}{\sqrt{\sum_{\pi \in \mathcal{P}(s_i, s'_i)} F(\pi) \sigma^{-\pi} \sum_{\theta \in \mathcal{P}(s_j, s'_j)} F(\theta) \sigma^{-\theta}}}. \quad (247)$$

The terms under the square-root are non-negative. To see that, let  $\pi = \alpha \circ \beta'$  be a path from  $s_i$  to  $s'_i$ . Then we know, that also  $\beta \circ \alpha'$ ,  $\alpha \circ \alpha'$  and  $\beta \circ \beta'$  exist and all go from  $s_i$  to  $s'_i$ . Thus, in  $G_{ii}$  we always find the four terms

$$R := \frac{F(\alpha \circ \beta')}{\sigma^{\text{len } \alpha} \bar{\sigma}^{\text{len } \beta}} + \frac{F(\beta \circ \alpha')}{\sigma^{\text{len } \beta} \bar{\sigma}^{\text{len } \alpha}} + \frac{F(\alpha \circ \alpha')}{\sigma^{\text{len } \alpha} \bar{\sigma}^{\text{len } \alpha}} + \frac{F(\beta \circ \beta')}{\sigma^{\text{len } \beta} \bar{\sigma}^{\text{len } \beta}} \quad (248)$$

together. So it is sufficient to show, that  $R$  is non-negative. With  $A := F(\alpha)/\sigma^{\text{len } \alpha}$  and  $B := F(\beta)/\sigma^{\text{len } \beta}$  we can rewrite  $R$  as

$$R = A\bar{B} + B\bar{A} + A\bar{A} + B\bar{B}. \quad (249)$$

With  $A = x + iy$  and  $B = u + iv$  we find

$$R = (x + u)^2 + (y + v)^2 \geq 0. \quad (250)$$

The same holds for  $G_{jj}$ .

We now proceed with (247). As we want to take the limit  $|\sigma| \rightarrow \infty$ , the smallest powers of  $\sigma$  will be dominant. The smallest powers of  $\sigma$  correspond to the shortest paths. We neglect higher orders and the asymptotic behaviour

$$\mu_{ij}(\sigma) \simeq \frac{|F(\eta_{ij'}) \sigma^{-\eta_{ij'}}|}{\sqrt{F(\eta_{ii'}) F(\eta_{jj'}) \sigma^{-(\eta_{ii'} + \eta_{jj'})}} \quad (251)$$

where we use the sign “ $\simeq$ ” to denote the asymptotic behaviour for  $|\sigma| \rightarrow \infty$ . Since the path  $\eta_{ii'}$  is always symmetric in the sense  $(\eta_{ii'})' = \eta_{ii'}$  we find  $\sigma^{-\eta_{ii'}} = |\sigma|^{\text{len}(\eta_{ii'})}$ . The same holds for  $\eta_{jj'}$ . With this we get

$$\mu_{ij}(s) \simeq \frac{|F(\eta_{ij'})|}{\sqrt{F(\eta_{ii'})F(\eta_{jj'})}} |\sigma|^{\frac{1}{2}(\text{len}(\eta_{ii'}) + \text{len}(\eta_{jj'})) - \text{len}(\eta_{ij'})}. \quad (252)$$

From lemma 37 we know, that the exponent of  $|s|$  is always non-negative, thus the limit always exists. If the lemma holds with equality, then the exponent equals zero and we get

$$\mu_{ij}(\sigma) \simeq \frac{|F(\eta_{ij'})|}{\sqrt{F(\eta_{ii'})F(\eta_{jj'})}}. \quad (253)$$

If inequality holds, then the exponent of  $|\sigma|$  is negative and we find

$$\lim_{|\sigma| \rightarrow \infty} \mu_{ij}(\sigma) = 0. \quad (254)$$

□

## F Spark - Mutual Coherence Inequality

As a final result we will show that the spark-mutual coherence inequality that has already been presented for the static problem in [10] stays valid for the gammoid of a linear dynamic system. In the proof for the static problem, one utilizes the Gershgorin circle theorem.

For the dynamic problem we can do a similar approach locally, meaning we get an inequality at each point  $\sigma \in \mathbb{C}$  in the complex plain. We will first show, that the it makes sense to consider the *generic rank* instead of the standard rank of the transfer function  $T$ . This will help us to finally deduce a global inequality.

### F.1 Eigenvalues of the Gramian

Let  $T : \mathbb{C} \rightarrow \mathbb{C}^{P \times M}$  be the transfer function of a linear dynamic system. One knows, that  $T$  has singularities at the eigenvalues of  $A$  (see section 6. E.1), but these will cause no issue for the following calculations. Assume for an  $\sigma_0 \in \mathbb{C}$  we find the rank

$$\text{rank } T(\sigma) = r < M. \quad (255)$$

If we regard  $T(\sigma) = (\mathbf{t}_1(\sigma), \dots, \mathbf{t}_M(\sigma))$  as a set of column vectors, then  $\{\mathbf{t}_1(\sigma_0), \dots, \mathbf{t}_M(\sigma_0)\}$  is a linearly dependent set of vectors. This can have two reasons. Either,  $\{\mathbf{t}_1, \dots, \mathbf{t}_M\}$

as function are linearly dependent, say of rank  $r$ . Then it is clear, that the rank of  $T(\sigma)$  will never exceed  $r$ . Or,  $\{\mathbf{t}_1, \dots, \mathbf{t}_M\}$  is a set of linearly independent functions, and the linear dependence at  $\sigma_0$  is just an unfortunate coincidence. In this case, for any  $\sigma$  in a vicinity of  $\sigma_0$ , we will find that the rank of  $T(\sigma)$  is  $M$  almost everywhere. For this reason, one defines the *structural* [25] or *generic rank* [29] of  $T$  as

$$\text{Rank } T := \max_{\sigma \in \mathcal{C}} \text{rank } T(\sigma). \quad (256)$$

From linear algebra it is clear, that for a fixed  $\sigma \in \mathbb{C}$ , the equation

$$T(\sigma) \tilde{\mathbf{w}}(\sigma) = \tilde{\mathbf{y}}(\sigma) \quad (257)$$

can be solved for  $\tilde{\mathbf{w}}(\sigma)$  if the rank of  $T(\sigma)$  equals  $M$ . From the argumentation above it becomes clear, that a generic rank of  $M$  already renders the whole system invertible.

Now, we formulate the well known Gershgorin theorem [18] in a form suitable for our purpose.

LEMMA 39: *Consider a complex matrix  $G: \mathbb{C} \rightarrow \mathbb{C}^{M \times M}$ . We call  $G$  strict diagonal dominant in  $\sigma$  if for all  $i = 1, \dots, M$  we find*

$$|G(\sigma)_{ii}| > \sum_{j \neq i} |G(\sigma)_{ij}|. \quad (258)$$

*If  $G$  is strict diagonal dominant in  $\sigma$ , then zero is not an eigenvalue of  $G(\sigma)$ .*

*Proof.* For a fixed  $\sigma$  set  $A := G(\sigma)$ . Assume  $\lambda \in \mathbb{C}$  is an eigenvalue of  $A$  with eigenvector  $\mathbf{v} \in \mathbb{C}^M$ . Let  $v_i$  be a component of  $\mathbf{v}$  of maximal magnitude, i.e.  $|v_i| \geq |v_j|$  for all  $j = 1, \dots, M$ . Without loss of generality we assume  $v_i = 1$ . We write the eigenvalue equation in components

$$\sum_{j=1}^M A_{ij} v_j = \lambda v_i. \quad (259)$$

We extract  $j = i$  from the sum to get

$$\sum_{j \neq i} A_{ij} v_j = \lambda - A_{ii}. \quad (260)$$

Taking the absolute value and applying the triangle inequality yields

$$|\lambda - A_{ii}| \leq \sum_{j \neq i} |A_{ij}| |v_j|. \quad (261)$$

By constrictioin  $|\nu_j| \leq |\nu_i| = 1$  thus we get the final result

$$|\lambda - A_{ii}| \leq \sum_{j \neq i} |A_{ij}|. \quad (262)$$

With  $r_i = \sum_{j \neq i} |A_{ij}|$  we can give a boundary of the spectrum  $\text{spec}(A)$  via a union of circles in the complex plane,

$$\text{spec}(A) \subseteq \bigcup_{i=1}^M \{\lambda \in \mathbb{C} \mid |\lambda - A_{ii}| \leq r_i\}. \quad (263)$$

Note that a strict diagonal dominant matrix necessarily has diagonal elements  $|A_{ii}| > 0$ . Furthermore  $A_{ii} > r_i$  for each  $i = 1, \dots, M$  and thus

$$0 \notin \{\lambda \in \mathbb{C} \mid |\lambda - A_{ii}| \leq r_i\}. \quad (264)$$

Consequently  $0 \notin \text{spec}(A)$ . □

Note, that the diagonal element of an input gramian  $G_{ii}$  is given by

$$G_{ij}(\sigma) = \sum_{j=1}^P T_{ij}^*(\sigma) T_{ji}(\sigma) = \sum_{j=1}^P |T_{ji}(\sigma)|^2 \quad (265)$$

and thus it is the zero function if and only if each  $T_{ji}$  for  $j = 1, \dots, P$  is the zero function. Again consider the dynamic system

$$T(\sigma) \tilde{w}(\sigma) = \tilde{y}(\sigma). \quad (266)$$

If the  $i$ -th column of  $T(\sigma)$  is zero for all  $\sigma \in \mathbb{C}$ , then  $\tilde{w}_i$  has no influence on the output at all. It is therefore trivially impossible to gain any information about  $\tilde{w}_i$ . We want to exclude this trivial case from our investigation and henceforth assume, that the diagonal elements of  $G$  are non-zero. By construction it is clear, that each diagonal element  $G_{ii}(\sigma)$  is indeed a positive real number.

## F.2 Strict Diagonal Dominance

Consider a linear dynamic input-output system with input set  $S = \{s_1, \dots, s_M\}$  and input gramian  $G : \mathbb{C} \rightarrow \mathbb{C}^{M \times M}$  and recall the definition of the coherence between input nodes  $s_i$  and  $s_j$

$$\mu_{ij}(\sigma) := \frac{|G_{ij}(\sigma)|}{\sqrt{G_{ii}(\sigma)G_{jj}(\sigma)}}. \quad (267)$$

The mutual coherence at  $\sigma$  is defined as

$$\mu(\sigma) := \max_{i \neq j} \mu_{ij}(\sigma). \quad (268)$$

For the special case, that the transfer function  $T$  is constant and real, this coincides with the definition of the mutual coherence from [10]. Also from there we take the following theorem and show that it stays valid for the dynamic problem.

**PROPOSITION 40:** *Consider a linear dynamic input-output system with input set  $S = \{s_1, \dots, s_M\}$ , input gramian  $G$ . Let  $\sigma \in \mathbb{C}$  and  $\mu(\sigma)$  the mutual coherence in  $\sigma$ . If the inequality*

$$G_{ii}(s) > \mu(s) \quad (269)$$

*holds for  $i = 1, \dots, M$ , then  $G$  is strictly diagonally dominant at  $s$ .*

*Proof.* First, rescale the system by

$$G(\sigma) \rightsquigarrow \frac{G(\sigma)}{\text{tr } G(\sigma)} \quad (270)$$

which gives the property

$$\sum_{i=1}^M G_{ii}(\sigma) = 1. \quad (271)$$

Note, that  $G_{ii}(\sigma) > 0$  is already clear and from the equation above  $G_{ii} < 1$ . The case  $M = 1$  is trivial. By definition for all  $i, j = 1, \dots, M$  with  $i \neq j$

$$|G_{ij}(\sigma)| \leq \mu(\sigma) \sqrt{G_{ii}(\sigma) G_{jj}(\sigma)}. \quad (272)$$

By assumption of the proposition  $\mu(\sigma) \leq G_{ii}(\sigma)$  for all  $i = 1, \dots, M$ , and since all quantities are non-negative

$$\mu < \sqrt{G_{ii}(\sigma) G_{jj}(\sigma)} \quad (273)$$

for all  $i \neq j$ . Combine the latter two inequalities and sum over all  $j = 1, \dots, i-1, i+1, \dots, M$  to get

$$\sum_{j \neq i} |G_{ij}(\sigma)| < G_{ii}(\sigma) \sum_{j \neq i} G_{jj}(\sigma) \quad (274)$$

for all  $i, \dots, M$ . Due to equation (271), the sum on the right hand side is smaller than one, thus for all  $i = 1, \dots, M$  we find

$$\sum_{j \neq i} |G_{ij}(\sigma)| < G_{ii}(\sigma) \quad (275)$$

which is exactly the definition of strict diagonal dominance at  $\sigma$ .  $\square$



### F.3 A note on the Coherence

In contrast to the static problem, where the coherence is a constant, we have here a function in the complex plane. Say, we have a small input set  $S = \{s_1, s_2\}$ . It is possible, that  $s_1$  and  $s_2$  are coherent in one regime of  $\mathbb{C}$  but will be incoherent in another. Proposition 40 and lemma 39 show, that a small coherence in a single  $\sigma \in \mathbb{C}$  is sufficient to get a high generic rank, and by this invertibility of the system. To have a measure whether two nodes  $s_i$  and  $s_j$  are distinguishable somewhere in  $\mathbb{C}$  it makes sense to define the *global coherence*

$$\mu_{ij} := \inf_{\sigma \in \mathbb{C}} \mu_{ij}(\sigma). \quad (276)$$

It is easy to see that the inequality

$$\max_{i \neq j} \inf_{\sigma \in \mathbb{C}} \mu_{ij}(\sigma) \leq \inf_{\sigma \in \mathbb{C}} \max_{i \neq j} \mu_{ij}(\sigma) \quad (277)$$

holds, formulated in terms of the global coherence  $\mu_{ij}$  and mutual coherence  $\mu(\sigma)$

$$\max_{i \neq j} \mu_{ij} \leq \inf_{\sigma \in \mathbb{C}} \mu(\sigma). \quad (278)$$

Proposition 40 holds for the mutual coherence  $\mu(\sigma)$  at any  $\sigma \in \mathbb{C}$ . The least restrictive bound for strict diagonal dominance is obviously achieved for a small mutual coherence  $\mu(\sigma)$ , so we would like to compute the minimum or infimum of  $\mu(\sigma)$ , the *global mutual coherence*

$$\mu := \inf_{\sigma \in \mathbb{C}} \mu(\sigma). \quad (279)$$

The inequality above indicates, that small global coherences  $\mu_{ij}$  do not necessarily lead to a small global mutual coherence  $\mu$ . More precisely

$$\max_{i \neq j} \mu_{ij} \leq \mu. \quad (280)$$

As an example, consider three input nodes  $s_1, s_2$  and  $s_3$  and three subsets of the complex plane  $U, V, W \subseteq \mathbb{C}$ . It might happen that  $\mu_{12}(\sigma)|_U$  is small, let us assume it vanishes, and so do  $\mu_{23}(\sigma)|_V$  and  $\mu_{13}(\sigma)|_W$ . Thus, all global coherences are vanishingly small. However, if  $U, V$  and  $W$  do not intersect, the global coherences are attained at different regions in the complex plane which means, in  $U$  we can distinguish  $s_1$  from  $s_2$  but we cannot distinguish  $s_2$  from  $s_3$ , and the same for  $V$  and  $W$ .

### E.3.1 Shortest Path Coherence

We want to estimate the global mutual coherence by the *mutual shortest path coherence*

$$\mu^{\text{short}} := \lim_{|\sigma| \rightarrow \infty} \mu(\sigma). \quad (281)$$

which is clearly an upper bound for the global mutual coherence. In contrast to the non-commuting infimum and maximum operations, the proposition below shows, that the limit and the maximum operations commute. We find

$$\lim_{|\sigma| \rightarrow \infty} \max_{i \neq j} \mu_{ij}(\sigma) = \max_{i \neq j} \lim_{|\sigma| \rightarrow \infty} \mu_{ij}(\sigma) = \max_{i \neq j} \mu_{ij}^{\text{short}}. \quad (282)$$

The quantity on the right hand side,  $\mu_{ij}^{\text{short}}$  is the *shortest path coherence* between  $s_i$  and  $s_j$ , which already appeared in proposition 38.

PROPOSITION 41: *Let  $\mu_{ij}(\sigma)$  be the coherence of  $s_i$  and  $s_j$ . Then*

$$\lim_{|\sigma| \rightarrow \infty} \max_{i \neq j} \mu_{ij}(\sigma) = \max_{i \neq j} \lim_{|\sigma| \rightarrow \infty} \mu_{ij}(\sigma). \quad (283)$$

*Proof.* First note, that  $\mu_{ij}(\sigma)$  is continuous,  $0 \leq \mu_{ij}(\sigma) \leq 1$  and that any singularity of  $\mu_{ij}(\sigma)$  is removable. Furthermore we have already seen that each  $\mu_{ij}(\sigma)$  convergent with limit  $\mu_{ij}^{\text{short}}$  as  $|\sigma| \rightarrow \infty$ . Due to these convenient properties, the following setting is sufficient.

Let  $f_a : \mathbb{R}_{\geq 0} \rightarrow \mathbb{R}$  a family of continuous and bounded functions with  $a \in I$  where  $I$  is a finite index set. We want to show that

$$\lim_{x \rightarrow \infty} \max_{a \in I} f_a(x) = \max_{a \in I} \lim_{x \rightarrow \infty} f_a(x). \quad (284)$$

To see that, let  $M_a := \lim_{x \rightarrow \infty} f_a(x)$  and let  $a^* \in I$  such that  $M_{a^*} = \max_{a \in I} M_a$ . By definition of  $M_a$ , for any  $\epsilon > 0$  there is an  $x_a$  such that for all  $x > x_a$  we have

$$|f_a(x) - M_a| < \epsilon. \quad (285)$$

Set  $x_0 := \max_{a \in I} x_a$  such that we can use the same epsilon and  $x_0$  for all indices  $a$ . Let us divide  $I = I_0 \dot{\cup} I_1$  such that  $I_0$  contains all indices with  $M_a < M_{a^*}$  and  $I_1$  contains this indices with  $M_a = M_{a^*}$

Let us first consider all  $I_0$  and let us choose  $\epsilon$  such that

$$\epsilon < \frac{1}{2} |M_{a^*} - M_a| \quad (286)$$

for all  $a \in I_0$ . We can rewrite this as

$$M_a + \epsilon < M_{a^*} - \epsilon. \quad (287)$$

For this choice of  $\epsilon$  there is an  $x_0$  such that  $|f_a(x) - M_a| < \epsilon$  for  $x > x_0$ , i.e.,

$$f_a(x) \in (M_a - \epsilon, M_a + \epsilon) \quad (288)$$

an analogously

$$f_{a^*}(x) \in (M_{a^*} - \epsilon, M_{a^*} + \epsilon). \quad (289)$$

Due to our choice of epsilon these two intervals are disjoint and one can see that  $f_a(x) < f_{a^*}(x)$  for all  $x > x_0$ . Thus for  $x$  large enough we can always neglect  $I_0$ ,

$$\max_{a \in I} f_a(x) = \max_{a \in I_1} f_a(x). \quad (290)$$

Let us now focus on  $I_1$ . Consider

$$r_a(x) := |f_a(x) - M_{a^*}| \quad (291)$$

for  $a \in I_1$  and let  $a' \in I_1$  such that  $f_{a'}(x) = \max_{a \in I_1} f_a(x)$ . It is now clear that

$$r_{a'}(x) \leq \max_{a \in I_1} r_a(x) \quad (292)$$

for all  $x$ . Insertion of the definitions yields

$$|f_{a'}(x) - M_{a^*}| \leq \max_{a \in I_1} |f_a(x) - M_{a^*}| \quad (293)$$

and for  $x > x_0$  we deduce

$$|f_{a'}(x) - M_{a^*}| < \epsilon. \quad (294)$$

Since we can do that for arbitrary small  $\epsilon > 0$  we find the convergence

$$\lim_{x \rightarrow \infty} f_{a'}(x) = M_{a^*}. \quad (295)$$

We can now insert the definitions

$$f_{a'}(x) = \max_{a \in I_1} f_a(x) = \max_{a \in I} f_a(x) \quad (296)$$

and

$$M_{a^*} = \max_{a \in I} M_a = \max_{a \in I} \lim_{x \rightarrow \infty} f_a(x) \quad (297)$$

to get the desired result

$$\lim_{x \rightarrow \infty} \max_{a \in I} f_a(x) = \max_{a \in I} \lim_{x \rightarrow \infty} f_a(x). \quad (298)$$

□

### E.3.2 Feed-Forward Graphs

As one special case we want to consider systems with a feed-forward structure. Such a structure for instance appears in artificial neural networks. From the matroid theory side, such systems correspond to cascade gammoids which were investigated in [26].

A gammoid  $\Gamma = (\mathcal{L}, g, \mathcal{M})$  is called a *cascade* if it has the following structure. The graph  $g = (\mathcal{N}, \mathcal{E})$  consists of a disjoint union of  $L + 1$  node sets

$$\mathcal{N} = \mathcal{N}_0 \dot{\cup} \dots \dot{\cup} \mathcal{N}_L \quad (299)$$

called layers. With  $(i, l)$  we mean node  $i$  from layer  $\mathcal{N}_l$ . Each edge in  $\mathcal{E}$  has the form

$$(i, l) \rightarrow (j, l + 1). \quad (300)$$

The input and output ground sets are set to be  $\mathcal{L} = \mathcal{N}_0$  and  $\mathcal{M} = \mathcal{N}_L$ .

In a cascade, all paths from the input layer to the output layer have the same length. For  $(i, 0) \in \mathcal{L}$  and  $(j, L) \in \mathcal{M}$  we find the transfer function to be

$$T_{ji}(\sigma) = \frac{1}{\sigma^L} \sum_{\pi \in \mathcal{P}((i,0),(j,L))} F(\pi) \quad (301)$$

One can see that

$$A_{ji} := \sum_{\pi \in \mathcal{P}((i,0),(j,L))} F(\pi) \quad (302)$$

defines the entries of a real constant matrix  $A$ . The transfer function achieves the simple form

$$T(\sigma) = \frac{1}{\sigma^L} A \quad (303)$$

and the coherence  $\mu_{ij}(\sigma)$  turns out to be a constant

$$\mu_{ij}(\sigma) = \frac{\langle a_i, a_j \rangle}{\|a_i\| \|a_j\|}. \quad (304)$$

The latter equation looks exactly like the coherence one defines for the static compressed sensing problem [10]. It follows, that for the class of cascade gammoids the different notions of coherence all coincide, and consequently the shortest path coherence indeed yields a method to compute the mutual coherence exactly.

## F.4 Estimation of the Spark

Also this calculation is in analogy to the static problem from [10]. Let  $G$  be the gramian of a linear dynamic input-output system with input set  $S = \{s_1, \dots, s_M\}$  and let  $\mu(\sigma)$  be its mutual coherence at  $\sigma \in \mathbb{C}$ . By the definition

$$|G_{ij}(\sigma)| \leq \mu(\sigma) \sqrt{G_{ii}(\sigma)G_{jj}(\sigma)}. \quad (305)$$

Now let  $G_{kk}(\sigma)$  be the maximum of all  $G_{ii}(\sigma)$  for  $i = 1, \dots, M$ . We replace the square root and sum over all  $j = 1, \dots, i-1, i+1, \dots, M$  to get

$$\sum_{j \neq i} |G_{ij}(\sigma)| \leq (M-1)\mu(\sigma)G_{kk}(\sigma), \quad (306)$$

where we used that the right hand side is independent of  $j$ . The gramian is strict diagonal dominant if for all  $i = 1, \dots, M$  we have

$$(M-1)\mu(\sigma)G_{kk}(\sigma) < G_{ii}(\sigma). \quad (307)$$

The latter inequality is therefore sufficient for strict diagonal dominance at  $\sigma$  and consequently to invertibility of the dynamic system. We therefore proceed with this inequality by using  $G_{ii}(\sigma)/G_{kk}(\sigma) < 1$  to get

$$M < \frac{1}{\mu(\sigma)} + 1. \quad (308)$$

Note, that the gammoid  $G$  depends on the choice of the input set  $S \subseteq \mathcal{L}$ . However, the sufficient condition for strict diagonal dominance only takes  $M = \text{card } S$  into account. It becomes clear, that for all  $\tilde{S} \subseteq \mathcal{L}$  with  $\text{card } \tilde{S} \leq M$  we get strict diagonal dominance. Since strict diagonal dominance leads to invertibility, it also tells us that  $\tilde{S}$  is independent  $\Gamma$ . By definition of the spark,  $\text{spark } \Gamma$  is the largest integer such that  $\tilde{S}$  is independent in  $\Gamma$  whenever  $\text{card } \tilde{S} \leq \text{spark } \Gamma$ . Since any  $M$  that fulfils (308) leads to independence, it becomes clear, that the spark is not smaller than the right hand side of this inequality. Therefore

$$\text{spark } \Gamma \geq \frac{1}{\mu(\sigma)} + 1. \quad (309)$$

The tightest bound for the spark is attained for the global mutual coherence  $\mu$ . In practice, however, we have to use the limit  $|\sigma| \rightarrow \infty$  and rely on the shortest path coherence.

## References

- [1] G. Basile and G. Marrq. A new characterization of some structural properties of linear systems: unknown-input observability, invertibility and functional controllability. *International Journal of Control*, 17(5):931–943, May 1973.
- [2] J. Bergh and Jorgen Lofstrom. *Interpolation Spaces: An Introduction*. Grundlehren der mathematischen Wissenschaften. Springer-Verlag, Berlin Heidelberg, 1976.
- [3] M. Blanke, M. Kinnaert, J. Lunze, and M. Staroswiecki. *Diagnosis and Fault-Tolerant Control*. Springer, Heidelberg, Germany, 2016.
- [4] Steven L. Brunton, Joshua L. Proctor, and J. Nathan Kutz. Discovering governing equations from data by sparse identification of nonlinear dynamical systems. *Proc Natl Acad Sci USA*, 113(15):3932–3937, April 2016.
- [5] E.J. Candes, J. Romberg, and T. Tao. Robust uncertainty principles: exact signal reconstruction from highly incomplete frequency information. *IEEE Transactions on Information Theory*, 52(2):489–509, February 2006.
- [6] E.J. Candes and T. Tao. Decoding by linear programming. *IEEE Transactions on Information Theory*, 51(12):4203–4215, December 2005.
- [7] Emmanuel J. Candès. The restricted isometry property and its implications for compressed sensing. *Comptes Rendus Mathematique*, 346(9):589–592, May 2008.
- [8] Kathleen Champion, Bethany Lusch, J. Nathan Kutz, and Steven L. Brunton. Data-driven discovery of coordinates and governing equations. *Proc Natl Acad Sci USA*, 116(45):22445–22451, November 2019.
- [9] D. L. Donoho. Compressed sensing. *IEEE Transactions on Information Theory*, 52(4):1289–1306, April 2006.
- [10] David L. Donoho and Michael Elad. Optimally sparse representation in general (nonorthogonal) dictionaries via l1 minimization. *Proceedings of the National Academy of Sciences*, 100(5):2197–2202, March 2003.
- [11] David L. Donoho and Philip B. Stark. Uncertainty Principles and Signal Recovery. *SIAM Journal on Applied Mathematics*, 49(3):906–931, June 1989.

- [12] Benjamin Engelhardt, Holger Fröhlich, and Maik Kschischo. Learning (from) the errors of a systems biology model. *Scientific Reports*, 6, November 2016.
- [13] Benjamin Engelhardt, Maik Kschischo, and Holger Fröhlich. A Bayesian approach to estimating hidden variables as well as missing and wrong molecular interactions in ordinary differential equation-based mathematical models. *Journal of The Royal Society Interface*, 14(131):20170332, June 2017.
- [14] M. Fliess. Nonlinear Control Theory and Differential Algebra: Some Illustrative Examples. *IFAC Proceedings Volumes*, 20(5, Part 8):103–107, July 1987.
- [15] Michel Fliess. A note on the invertibility of nonlinear input-output differential systems. *Systems & Control Letters*, 8(2):147–151, December 1986.
- [16] Simon Foucart and Holger Rauhut. *A Mathematical Introduction to Compressive Sensing*. Applied and Numerical Harmonic Analysis. Birkhauser Boston Inc., Cambridge, MA, 2013.
- [17] G Nakamura and R Potthast. *An introduction to the theory and methods of inverse problems and data assimilation*. IOP Publishing, Bristol, UK, 2015.
- [18] S. A. Gershgorin. Über die Abgrenzung der Eigenwerte einer Matrix. *Bulletin de l'Académie des Sciences de l'URSS. VII. Série*, 1931(6):749–754, 1931.
- [19] A. W Ingleton and M. J Piff. Gammoids and transversal matroids. *Journal of Combinatorial Theory, Series B*, 15(1):51–68, August 1973.
- [20] R. Isermann. *Fault-diagnosis applications*. Springer, Heidelberg, Germany, 2011.
- [21] Dominik Kahl, Philipp Wendland, Matthias Neidhardt, Andreas Weber, and Maik Kschischo. Structural invertibility and optimal sensor node placement for error and input reconstruction in dynamic systems. *Phys. Rev. X*, 9:041046, Dec 2019.
- [22] Matthias Kahm, Clara Navarrete, Vicent Llopis-Torregrosa, Rito Herrera, Lina Barreto, Lynne Yenush, Joaquin Ariño, Jose Ramos, and Maik Kschischo. Potassium Starvation in Yeast: Mechanisms of Homeostasis Revealed by Mathematical Modeling. *PLoS Computational Biology*, 8(6):1–11, June 2012.

- [23] Yang-Yu Liu and Albert-László Barabási. Control principles of complex systems. *Reviews of Modern Physics*, 88(3), September 2016.
- [24] David G. Luenberger. *Introduction to Dynamic Systems: Theory, Models, and Applications*. Wiley, Hoboken, NJ, USA, May 1979.
- [25] Jan Lunze. Einführung in die Mehrgrößenregelung. In *Regelungstechnik 2: Mehrgrößensysteme, Digitale Regelung*, Heidelberg, Germany, 2016. Springer Berlin Heidelberg.
- [26] J. H. Mason. On a Class of Matroids Arising From Paths in Graphs. *Proceedings of the London Mathematical Society*, s3-25(1):55–74, June 2018.
- [27] D. Joseph Mook and John L. Junkins. Minimum model error estimation for poorly modeled dynamic systems. *Journal of Guidance, Control, and Dynamics*, 11(3):256–261, 1988.
- [28] Jaime Moreno, Edmundo Rocha-Cozatl, and Alain Vande Wouwer. Observability/detectability analysis for nonlinear systems with unknown inputs - Application to biochemical processes. In *2012 20th Mediterranean Conference on Control and Automation, MED 2012 - Conference Proceedings*, pages 151–156, July 2012.
- [29] Kazuo Murota. *Matrices and Matroids for Systems Analysis*. Springer-Verlag Berlin Heidelberg, Heidelberg, Germany, October 2009.
- [30] Mark Newman. *Networks: An Introduction*. Oxford University Press, March 2010.
- [31] Devin N. Patel and Stephen J. Freedland. New Prostate Cancer Biomarkers: The Search Continues. *European Urology*, 72(6):950–951, December 2017.
- [32] Jaideep Pathak, Brian Hunt, Michelle Girvan, Zhixin Lu, and Edward Ott. Model-Free Prediction of Large Spatiotemporally Chaotic Systems from Data: A Reservoir Computing Approach. *Phys. Rev. Lett.*, 120(2):024102, January 2018.
- [33] Hazel Perfect. Applications of Menger’s graph theorem. *Journal of Mathematical Analysis and Applications*, 22(1):96–111, April 1968.
- [34] Hazel Perfect. Independence Spaces and Combinatorial Problems. *Proceedings of the London Mathematical Society*, s3-19(1):17–30, 1969.
- [35] J. S. Pym. The Linking of Sets in Graphs. *Journal of the London Mathematical Society*, s1-44(1):542–550, January 1969.



- [36] J. S. Pym. A proof of the linkage theorem. *Journal of Mathematical Analysis and Applications*, 27(3):636–638, September 1969.
- [37] M. Sain and J. Massey. Invertibility of linear time-invariant dynamical systems. *IEEE Transactions on Automatic Control*, 14(2):141–149, April 1969.
- [38] M. Schelker, A. Raue, J. Timmer, and C. Kreutz. Comprehensive estimation of input signals and dynamics in biochemical reaction networks. *Bioinformatics*, 28(18):i529–i534, September 2012.
- [39] L. Silverman. Inversion of multivariable linear systems. *IEEE Transactions on Automatic Control*, 14(3):270–276, 1969.
- [40] Eduardo D. Sontag. Mathematical Control Theory. In J. E. Marsden, L. Sirovich, M. Golubitsky, and W. Jäger, editors, *Texts in Applied Mathematics*, volume 6, New York, NY, 1998. Springer New York.
- [41] Nikolaos Tsiantis, Eva Balsa-Canto, and Julio R Banga. Optimality and identification of dynamic models in systems biology: an inverse optimal control framework. *Bioinformatics*, 34(14):2433–2440, July 2018.
- [42] G. Vossen and H. Maurer. OnL1-minimization in optimal control and applications to robotics. *Optimal Control Applications and Methods*, 27(6):301–321, November 2006.
- [43] Torsten Wey. Rank and Regular Invertibility of Nonlinear Systems: A Graph Theoretic Approach. *IFAC Proceedings Volumes*, 31(18):257–262, July 1998.
- [44] Hassler Whitney. On the Abstract Properties of Linear Dependence. *American Journal of Mathematics*, 57(3):509–533, 1935.
- [45] Or Yair, Ronen Talmon, Ronald R. Coifman, and Ioannis G. Kevrekidis. Reconstruction of normal forms by learning informed observation geometries from data. *Proc Natl Acad Sci USA*, 114(38):E7865–E7874, September 2017.
- [46] Yonina C. Eldar and Gitta Kutyniok. *Compressed Sensing*. Cambridge University Press, Cambridge, UK, 2012.